| |
|---|
| Other reference : |
| ESTEC/Contract N° 4000102571/10/NL/AF |
| Type : |
| |
| Description : |
| Radiation Characterization of LAPLACE/TANDEM RH Optocouplers, Sensors and Detectors |
| Title of document : |
| **HAS2 TID Report** |

| | Names | Dates |
|---|---|---|
| Prepared by | VAN AKEN Dirk (ON Semiconductor)<br>HERVE Dominique (Sodern)<br>BEAUMEL MATTHIEU (Sodern) | 23/11/2012 |
| Checked by | - | - |
| Approved by | - | - |
| Customer approval | - | - |

| ***CHANGE RECORD*** | |
|---|---|
| Revision | Description of change |
| A | First issue |
| B | Added witness part test results |

***TABLE OF CONTENTS***

# 1.SCOPE AND APPLICABILITY

## 1.1.Scope

This test report presents the results of the TID irradiation testing on the HAS2 CMOS image sensor, performed in the frame of the ESTEC contract N° 400 0102571/10/NL/AF "Radiation Characterization of Laplace/Tandem RH optocouplers, sensors and detectors".

The TID irradiations were performed at the ESTEC Co-60 source in October 2011. The annealing steps at room temperature and elevated temperatures were performed at ON Semiconductor.

## 1.2.Purpose

The effect of TID radiation and annealing is studied on the HAS2 in the ON and OFF state in all different possibilities such as ON during radiation and OFF during annealing etc...

# 2.REFERENCES

## 2.1.Applicable documents

[AD 1] ITT 6429 HAS Irradiation Test Plan, PR__00004584, D

## 2.2.Reference documents

[RD1] Radiation Test Summary

[RD2] HAS Low Dose Rate Radiation Test Report

[RD3] HAS TID Report 2007 Evaluation Campaign

# 3.ABBREVIATIONS

| | |
| --- | --- |
| AD | Applicable Document |
| APS | Active Pixel Sensor |
| CDS | Correlated Double Sampling |
| CMOS | Complementary Metal-Oxide Semiconductor |
| DC | DateCode |
| DDD | Displacement Damage Dose |
| DR | Destructive Readout |
| DS | Double Sampling |
| DSNU | Dark Signal Non Uniformity |
| ECSS | European Cooperation for Space Standardization |
| EOL | End Of Life |
| ESA | European Space Agency |
| FPN | Fixed Pattern Noise |
| HAS2 | High Accuracy STR 2 |
| LET | Linear Energy Transfer |
| LSB | Least Significant Bit |
| N/A | Not Applicable |
| NDR | Non-Destructive Readout |
| PCB | Printed Circuit Board |
| RD | Reference Document |
| SEE | Single Event Effect |
| SET | Single Event Transient |
| SEU | Single Event Upset |
| SEFI | Single Event Failure interrupt |
| TID | Total Ionizing Dose |

# 4. DEVICE INFORMATION

## 4.1. HAS2 presentation

The Accuracy STR 2 sensor (HAS2) is a 1024 x 1024 pixel rolling shutter Active Pixel Sensor (APS), featuring a programmable (gain and offset) output amplifier (PGA) and an internal 12 bits ADC.

The CMOS image was sensor designed and manufactured by ON Semiconductor[1] under ESA contract 17235/03/NL/FM for star tracker applications.

The block diagram of HAS2 is presented in Figure 4-1.

Pixel design is based on a photodiode coupled with a three transistor readout circuit. The HAS2 is the descendant from a lineage radiation-hardened by design sensors from ON Semiconductor: the photodiodes includes a doped surface protection layer to prevent the depleted area from reaching the field oxide interface, while the CMOS readout circuitry is designed using enclosed geometry transistor layouts.

The wafers are produced by Plessey Semiconductors[2] on the standard XC035P311 CMOS process (0.35 µm).

In order to reduce the variation in signal offset from pixel to pixel (known as Fixed Pattern Noise, or FPN) typically seen on APS, the HAS2 implements two different noise reduction techniques: Double Sampling (DS) also called Destructive Readout (DR) and Correlated Double Sampling (CDS) also called Non Destructive Readout (NDR). In DR mode, the pixel is reset at the end of the signal integration time in order to sample the pixel reference level. The reference level is subtracted from the signal level in order to cancel the pixel offset. This internal analog operation is performed before digitization. In NDR mode, two images are sampled and digitized: a reference image at the beginning of the integration time, and a signal image at its end. Offset correction must be performed off-chip by subtracting these two images.

A temperature sensor is also integrated on chip, which can be addressed through an internal multiplexer. This MUX can also address analogue inputs to be digitized by the internal ADC.

[1] Formerly Cypress BVBA and Fillfactory.
[2] Formerly X-FAB.

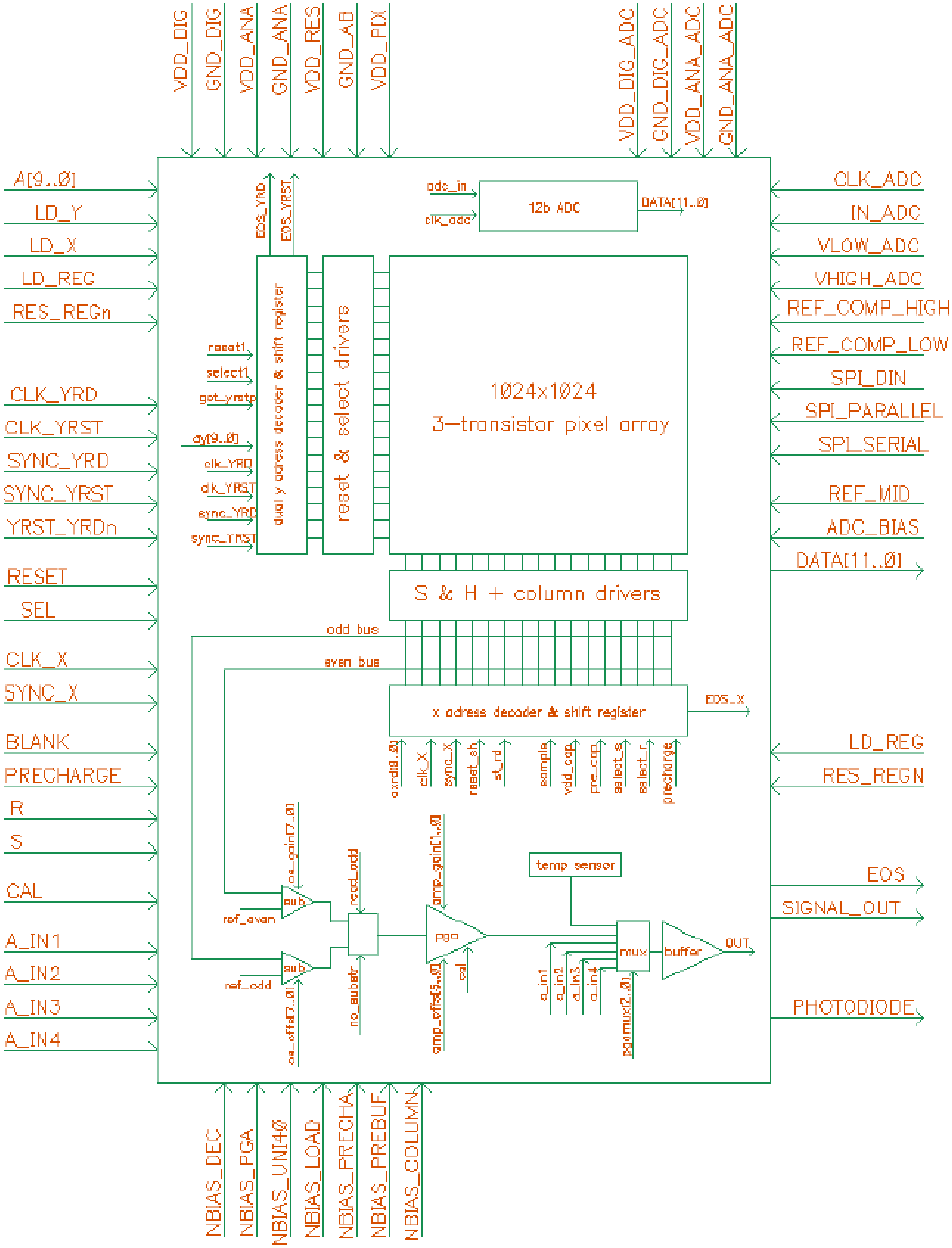


**Figure 4-1 : HAS2 block diagram**

## 4.2. Samples identification

Part type: HAS2
Manufacturer: ON Semiconductor
Package: JLCC84
Tested Samples:

164 Reference sample used during HAS ESCC evaluation campaign
689 Sample from wafer lot P29506.1
572 Sample from wafer lot P20291.1
698 Sample from wafer lot P29506.1
566 Sample from wafer lot P20291.1
713 Sample from wafer lot P29506.1
569 Sample from wafer lot P20291.1
688 Sample from wafer lot P29506.1
705 Sample from wafer lot P29506.1
717 Sample from wafer lot P29506.1
570 Sample from wafer lot P20291.1
679 Sample from wafer lot P29506.1
541 Sample from wafer lot P20291.1
580 Sample from wafer lot P20291.1
723 Sample from wafer lot P29506.1
741 Sample from wafer lot P29506.1
88 Sample from wafer lot P20291.1, 2007 ESCC evaluation lot
687 Sample from wafer lot P29506.1
739 Sample from wafer lot P29506.1
696 Sample from wafer lot P29506.1
576 Sample from wafer lot P20291.1
575 Sample from wafer lot P20291.1
73 Sample from wafer lot P20291.1, 2007 ESCC evaluation lot
731 Sample from wafer lot P29506.1
697 Sample from wafer lot P29506.1

Samples from wafer lot P29506.1:
Backside marking: NOIH2SM1000A HHC (Engineering Models)
Date code: 110414 (April 14, 2011)

Samples from wafer lot P20291.1:
Backside marking: NOIH2SM1000A HHC (Engineering Models)
Date code: 110414 (April 14, 2011)

Samples from wafer lot P29506.1 (2007:
Backside marking: NOIH2SM1000A HHC (Engineering Models)
Date code: 110414 (April 14, 2011)

Sample 679, 713 and 741 were taken out of the beam after 55.1KRad for later use during SEE testing.

All samples have been subjected to an operational burn in step at +125 degC during 168h.

# 5.IRRADIATION FACILITY

Radiations were perfomed at the ESTEC CO-60 radiation facility. Detailed information on the dosimetry can be found in the irradiation test campaign details report (ref. RD1).

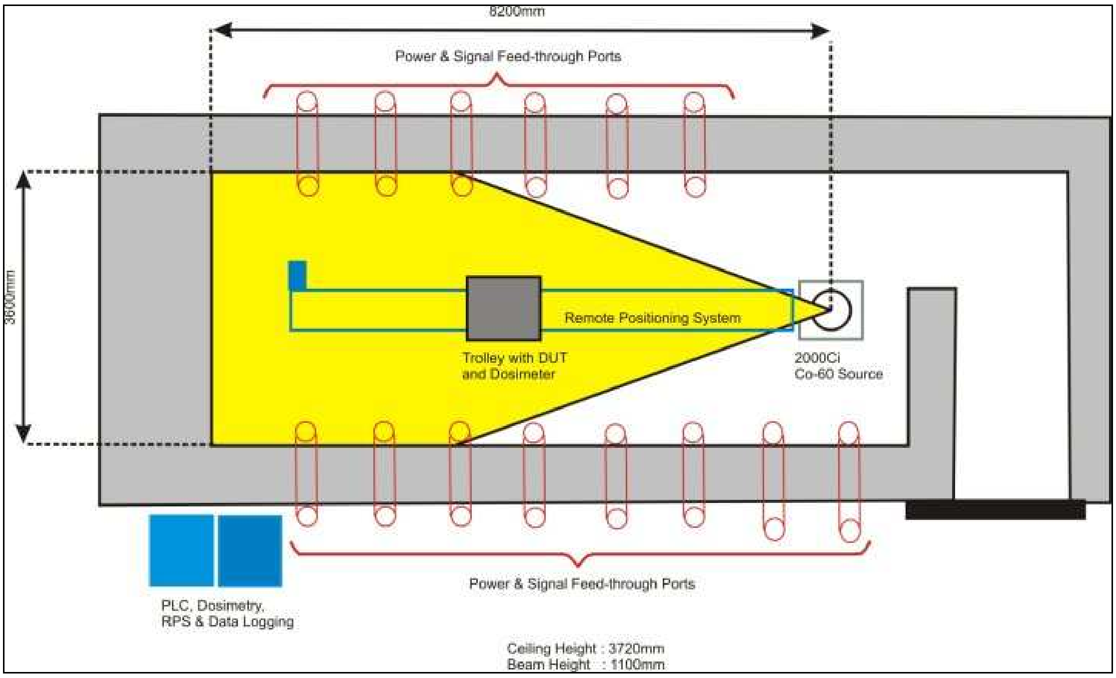


**Figure 5-1: ESA-ESTEC Co-60 radiation room layout**

# 6.TEST SETUP

The irradiations and electrical characterizations have been performed at room temperature. Image acquisition was done using dedicated driving boards and acquisition system.

The figure hereafter presents the geometry of the irradiation setup.

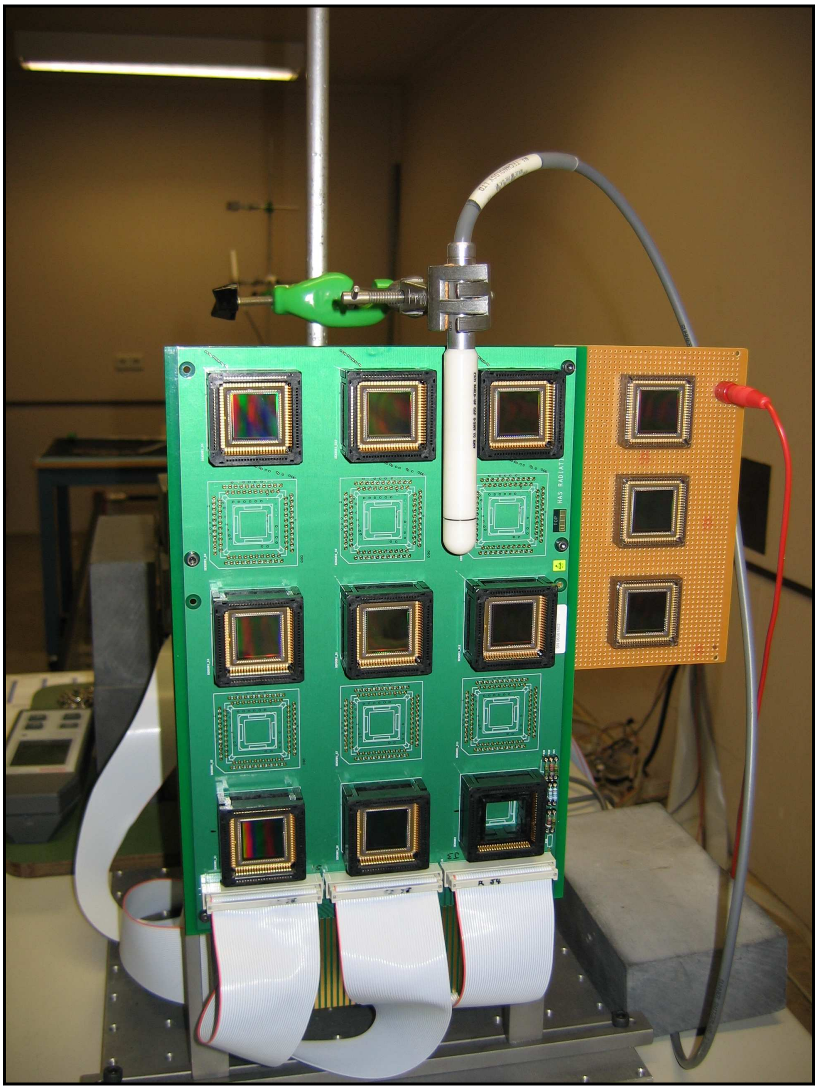

**Figure 6-1 : HAS Irradiation Test Setup**

The HAS2 is operated under beam in Soft Reset condition.

The camera system consists in 4 main components (Figure 6-2). The boards implemented in the system are detailed hereafter:

- A digital controller runs the image sensor controller, the frame grabber and the communication to a PC.
- A cable interface board contains the controllable power supplies, cable line drivers to drive the control signals to the DUT and receivers that receive the video signal from the DUT.

- A cable receiver board receives the driving signals from the controller and also contains buffers to drive the video signal to the 5 meter long cable.
- A radiation/burn-in board contains the DUT. The DUT returns a video signal to the controller.

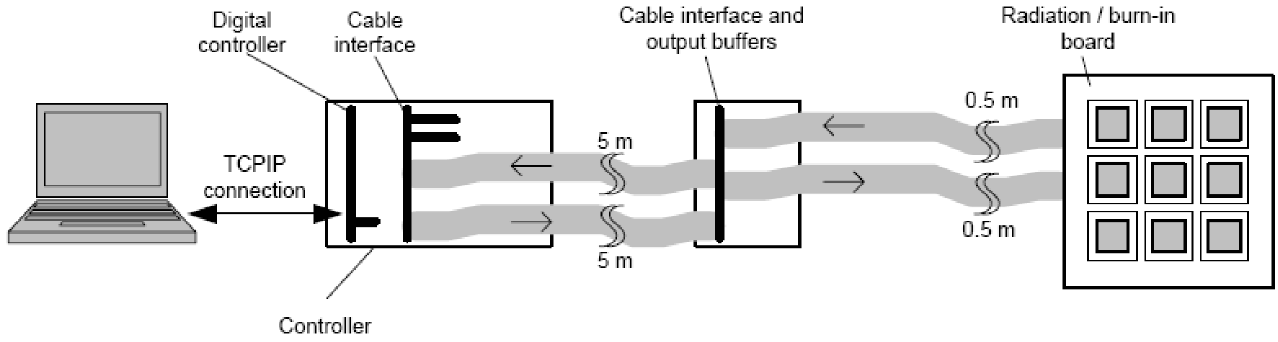


**Figure 6-2 : Overview of the HAS2 test setup**

During irradiation the device supply currents are monitored separately. In case of abnormal drift or device failure, the following parameters can be logged: power supply where the drift condition occurred, time when the condition occurred, and drift current. In case of latch-up the current supplied to the device is limited to a safe value in order to prevent damage.

# 7.Test Plan

Electrical measurements are performed at the following steps:

- Initial characterization
- 8.1 KRad
- 31.5 KRad
- 55.1 KRad
- 78.6 KRad
- 144.5 KRad
- 3 months room temperature annealing (measurements on a weekly basis)
- 1 month 50 degC annealing (measurements twice a week)
- 168 hours 1250 degC annealing (measurements every 24h)

Next to the electrical testing, electro optical testing is performed before radiation and after 144.5 KRad. Electro-optical testing is not performed after the two annealing steps.

Devices have been irradiated using the following bias conditions:

| Condition Item | Bias State during Irradiation test campaign | Bias state during Post irradiation annealing | Serial Numbers |
|---|---|---|---|
| A | ON | ON | 688, 717, 723 |
| A2 | ON | ON | 541, 566 |
| B | ON | OFF | 698, 705, |
| B2 | ON | OFF | 569, 570, 572 |
| C | OFF | ON | 689, 697, 731 |
| C2 | OFF | ON | 73, 575, 576 |
| D | OFF | OFF | 687, 696, 739 |
| D2 | OFF | OFF | 88, 580 |

The samples used for A, B, C and D are issued from the same wafer lot (ref. Section 2.4). The samples used for condition A2, B2, C2 and D2 are issued from the wafer lot used during the ESCC HAS2 evaluation campaign.

# 8. EXPERIMENTAL RESULTS

## 8.1. Reported parameters

The following electrical parameters are reported in the next paragraphs:

- Temporal noise in DR mode (hard reset, hard to soft reset)
- Temporal noise in NDR mode (hard reset, hard to soft reset)
- Offsets (in particular DR mode odd/even offset difference and NDR mode offset dispersion – mean, standard deviation, register value)
- Fixed pattern noise (FPN) local and global (hard reset, hard to soft reset)
- Dark current
- Dark current non uniformity local and global
- Photo response non uniformity local and global
- Temperature sensor output
- Supply currents
- ADC Performances (INL, DNL)

The following electro-optical parameters are measured:

- Spectral Response
- FTM
- Linearity and full well capacity
- Conversion factor
- Dark signal temperature dependency
- Lag performance

## 8.2. Observations

We have been facing quite some serious issues during the execution of the work. First of all there was the test equipment failure during the irradiation campaign at ESTEC. During the electrical tests in between the irradiation campaigns some strange behavior was observed on the parts: some of the parts were showing high operating current, other parts gave some contact test issues, some parts were showing zero dark current increase, and so on. By retesting the parts until good and expected data was achieved we could minimize the damage. Investigations later on pointed out that the issue was due to a broken contact pin which was probably introduced during the travel of the equipment from Belgium to ESTEC.

The second issue we had was the mix-up of integration time settings for the dark current image. The tester used for this test campaign was also used for the neutron irradiated devices and was also used for production testing. Every type of test required its own integration time setting for the dark current. Unfortunately this issue was only been seen during the 11$^{th}$ week of the room temperature annealing. But, as there was no difference seen between the first and the 11$^{th}$ week of the room temperature annealing, no crucial data have been lost!

The graphs which will be shown in the next paragraphs' needs to be interpreted with care due to the above.

### 8.2.1.Dark Current

The following graph is displaying the average dark current behavior of the 8 different biasing conditions.

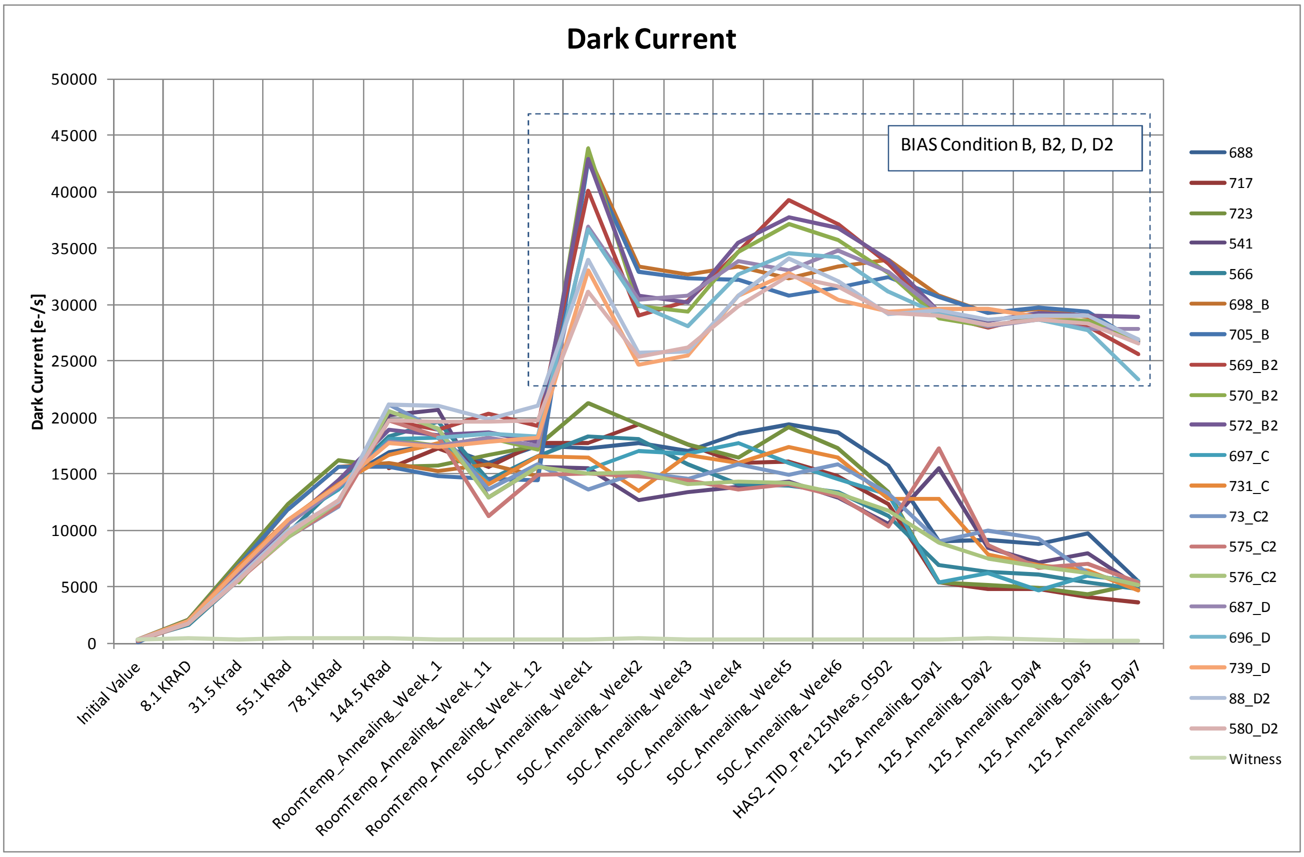


**Figure 8-1: Dark Current vs radiation and annealing for different bias conditions**

The following observations are made:

- Dark current increases the same for all the samples, independent from the wafer lot, independent from the biasing conditions.
- Dark current does not change significantly during room temperature annealing for the devices in the ON condition.
- Dark current increases significantly for after 1 day of 50 degrees C annealing for the OFF biasing condition (B, B2, D and D2), and is quite unstable during this annealing period.
- Dark current drops during 125degC annealing for both the biased and unbiased condition.

8.2.1.1. Distributions

The graph below is showing the DSNU distributions for device ID 88 which was in the OFF state during radiation and annealing. Please note that the below curves have an integration time of 3 seconds.

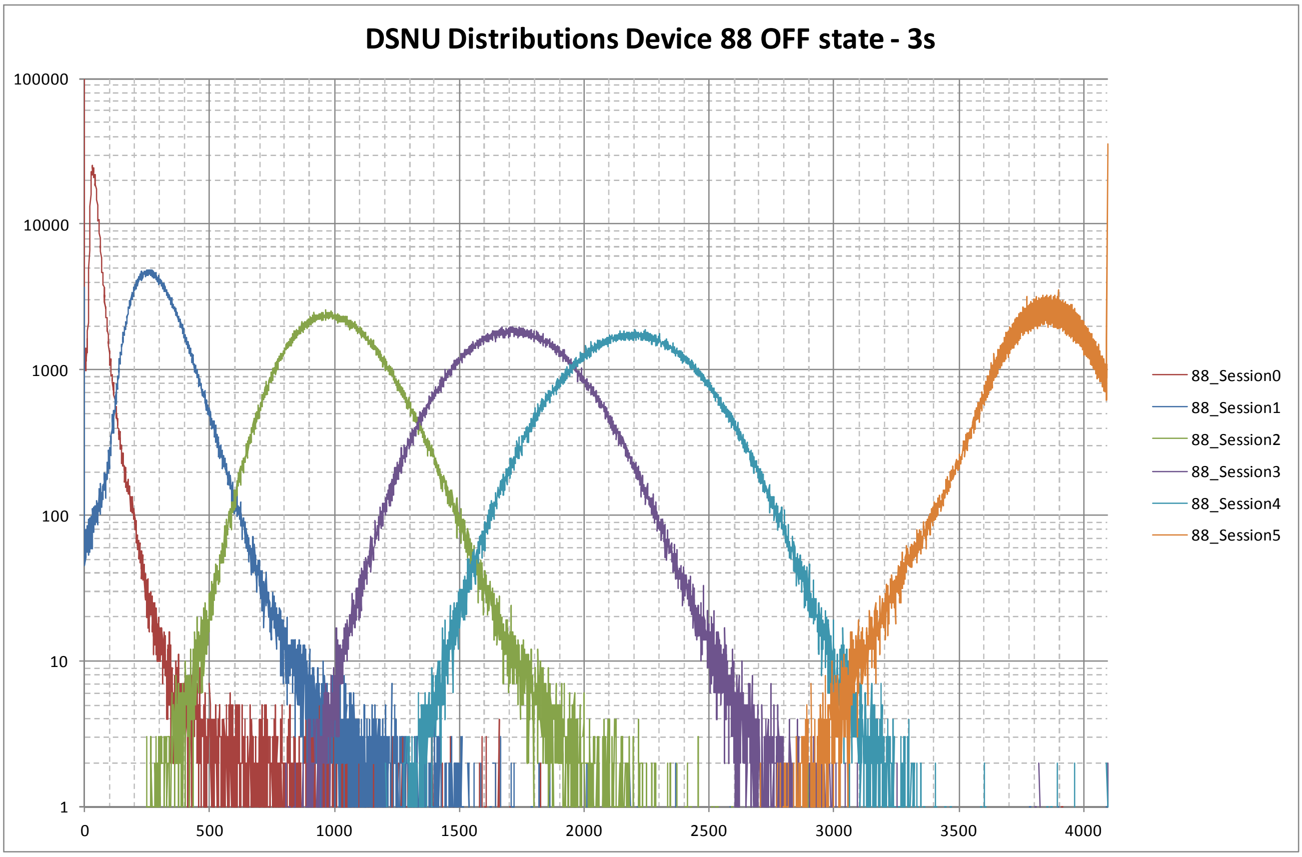


**Figure 8-2: DSNU distributions for device 88**

The next graph is also showing the DSNU distributions for device 88 but this time after room temperature, 50C and 125C annealing. For these distributions an integration time of 1 second was applied.

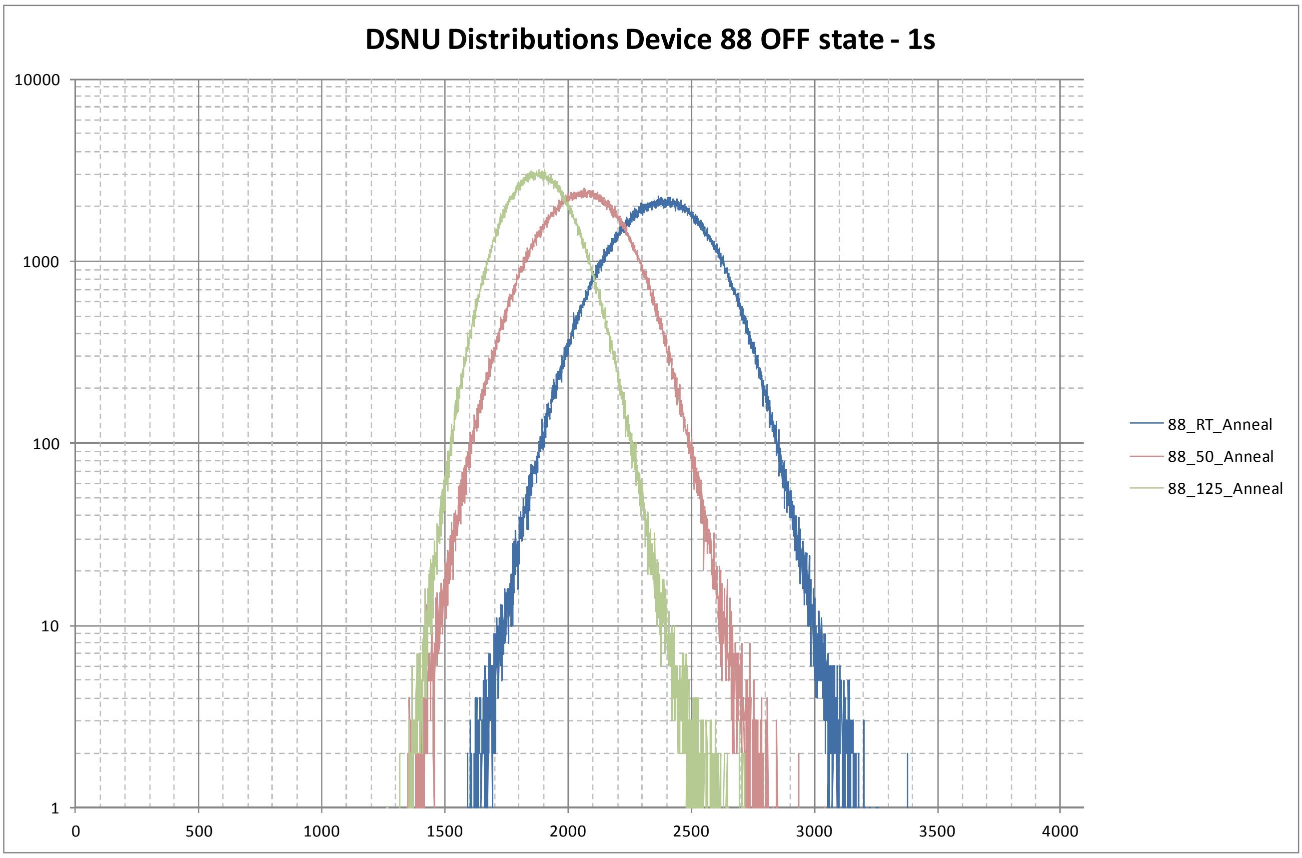


**Figure 8-3: DSNU distributions for device 88 after annealing**

The graph below is showing the DSNU distributions for device ID 566 which was in the ON state during radiation and annealing. Please note that the below curves have an integration time of 3 seconds.

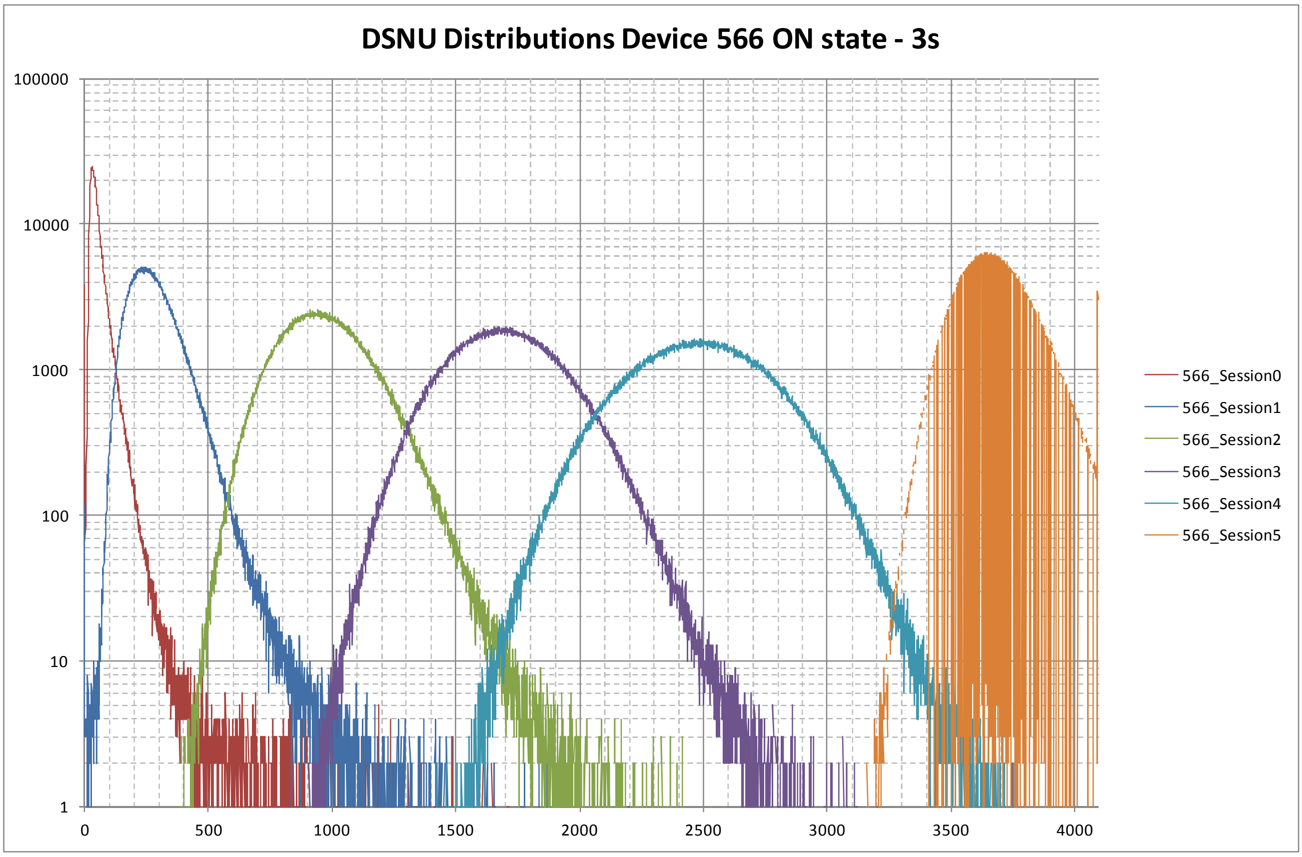


**Figure 8-4: DSNU distributions for device 566**

Please note that the session 5 distribution has some missing ADC codes due to a testing issue.

The next graph is also showing the DSNU distributions for device 566 but this time after room temperature, 50C and 125C annealing. For these distributions an integration time of 1 second was applied.

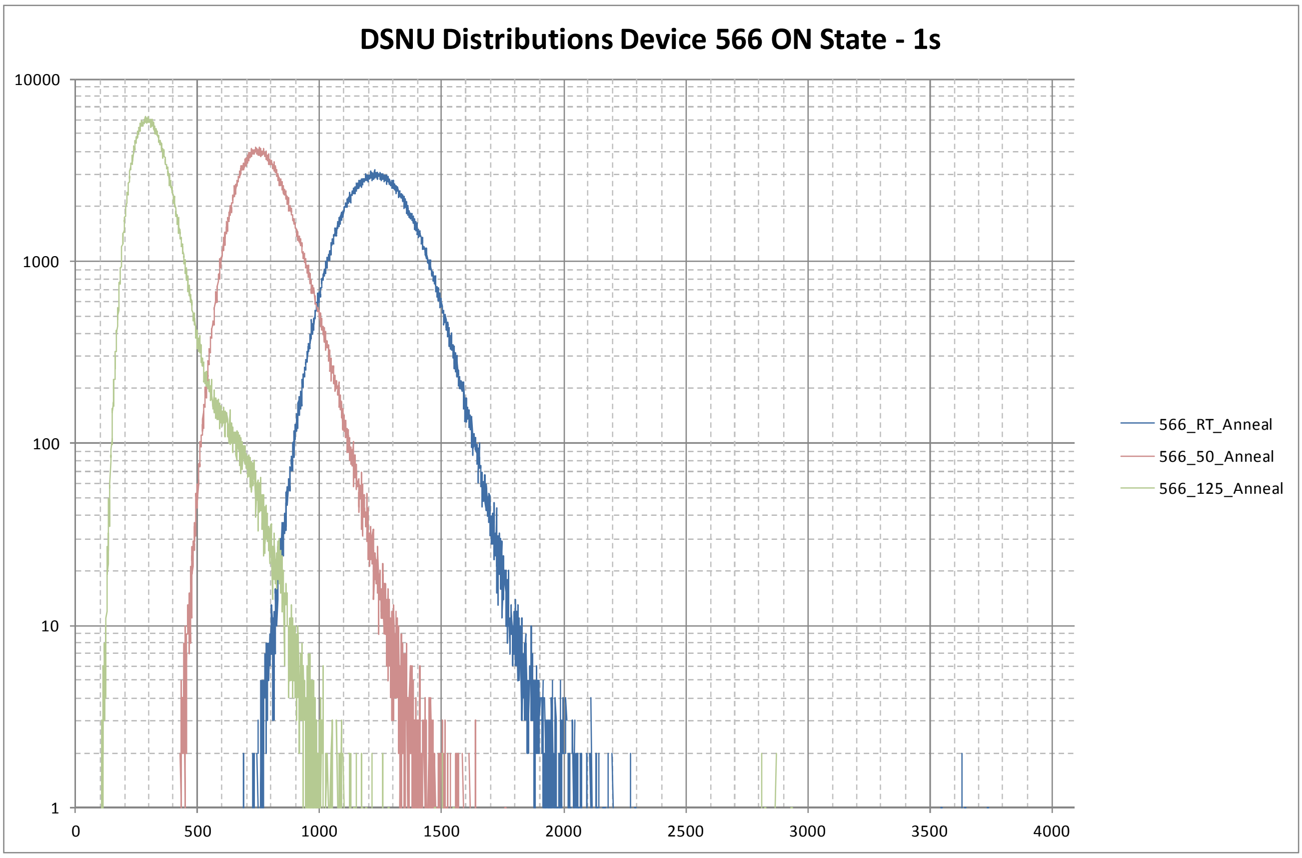


**Figure 8-5: DSNU distributions for device 566 after annealing**

### 8.2.2. Temporal Noise in DR Mode – hard reset

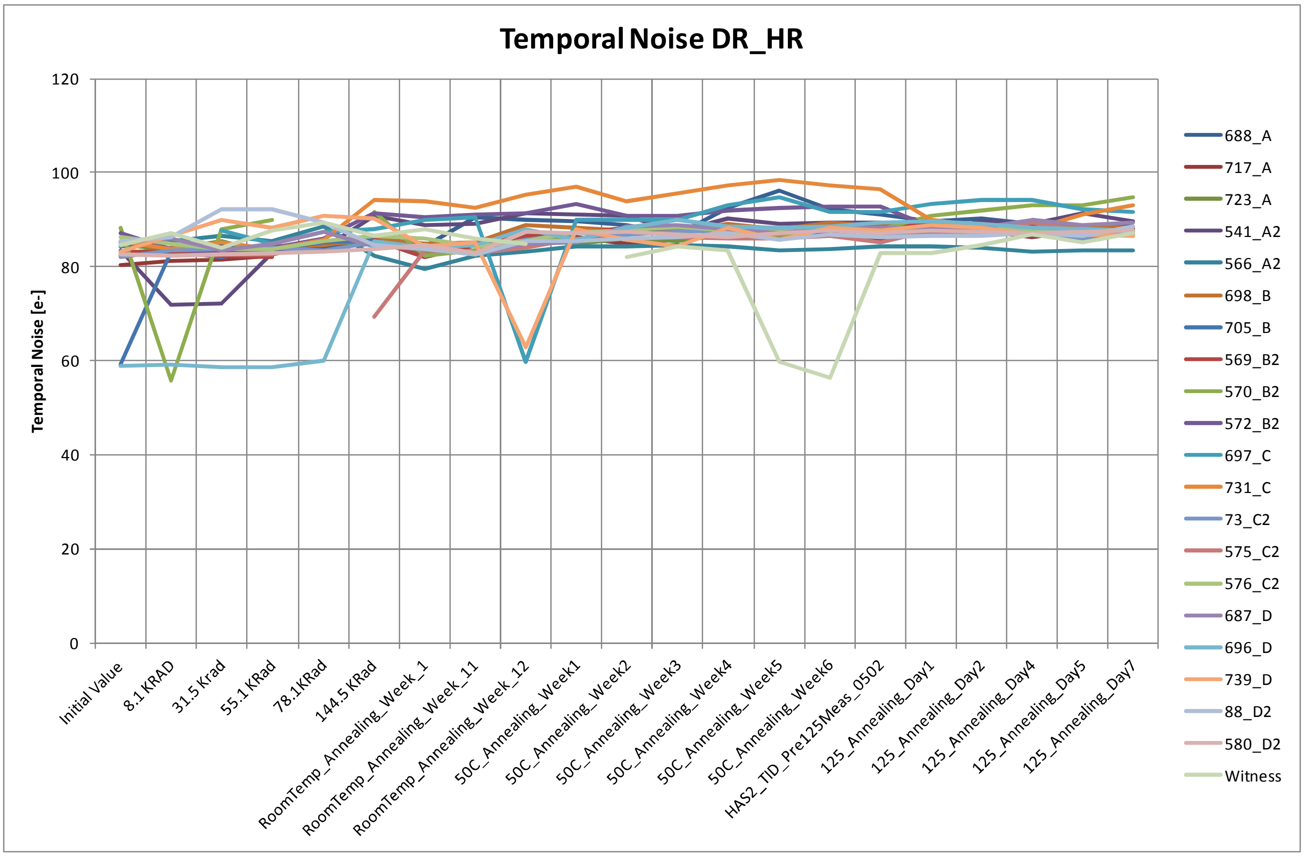


**Figure 8-6: Temporal Noise in DR mode – hard reset vs radiation and annealing**

The following observations are made:

- Some test points are not reliable due to tester instability during the radiation test.
- Taking an average over the different samples, there's no difference visible between radiation, room temperature annealing and high temperature annealing.
- There is no difference between the different biasing schemes.

### 8.2.3. Temporal Noise in DR Mode – hard to soft reset

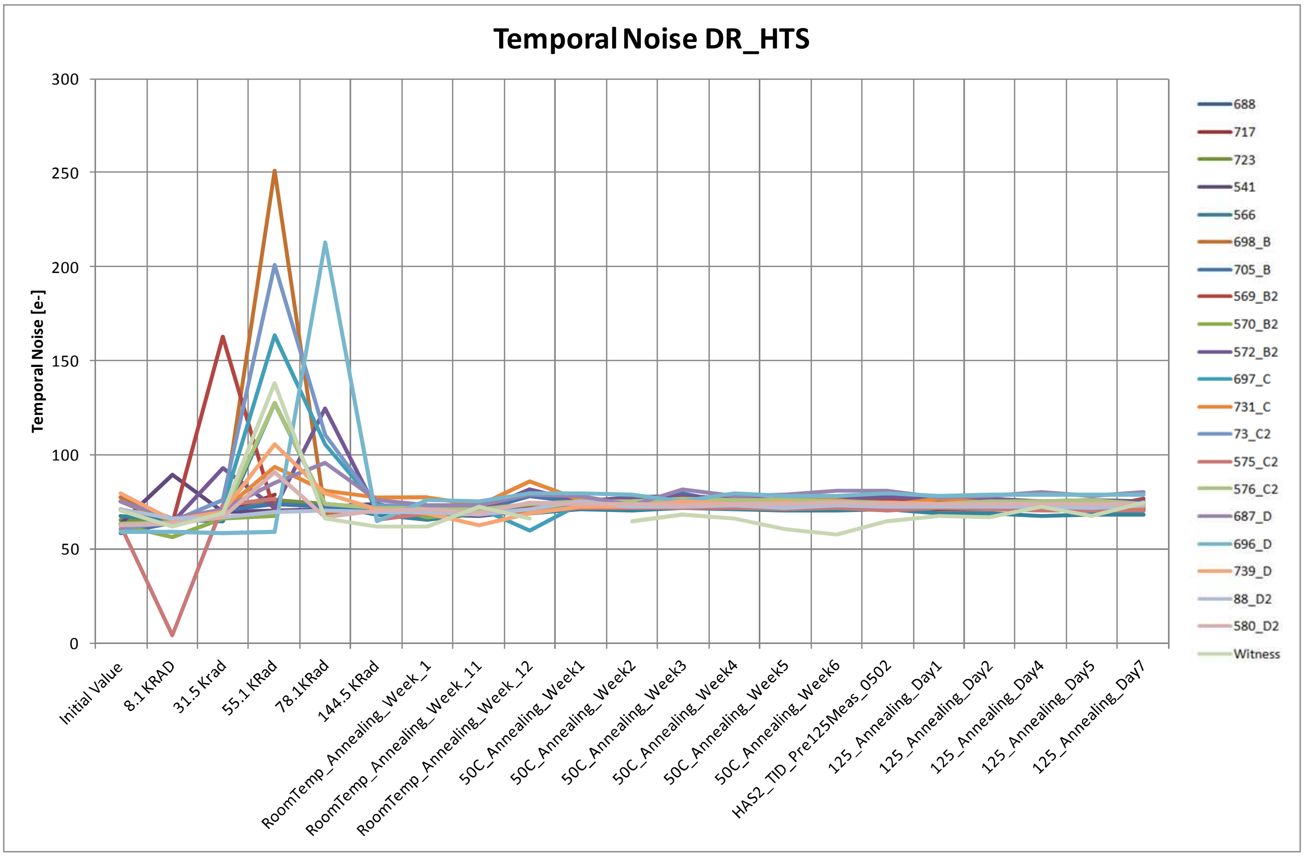


**Figure 8-7: Temporal Noise in DR mode – hard to soft reset vs radiation and annealing**

The following observations are made:

- Some test points are not reliable due to tester instability during the radiation test.
- Some of the measurement points obtained during irradiation are showing high values. The same effect was observed during the evaluation phase in 2007.
- During room temperature annealing and high temperature annealing there is no change in temporal noise.
- The temporal noise is the same amongst the different biasing schemes.

### 8.2.4. Temporal Noise in NDR Mode – hard reset

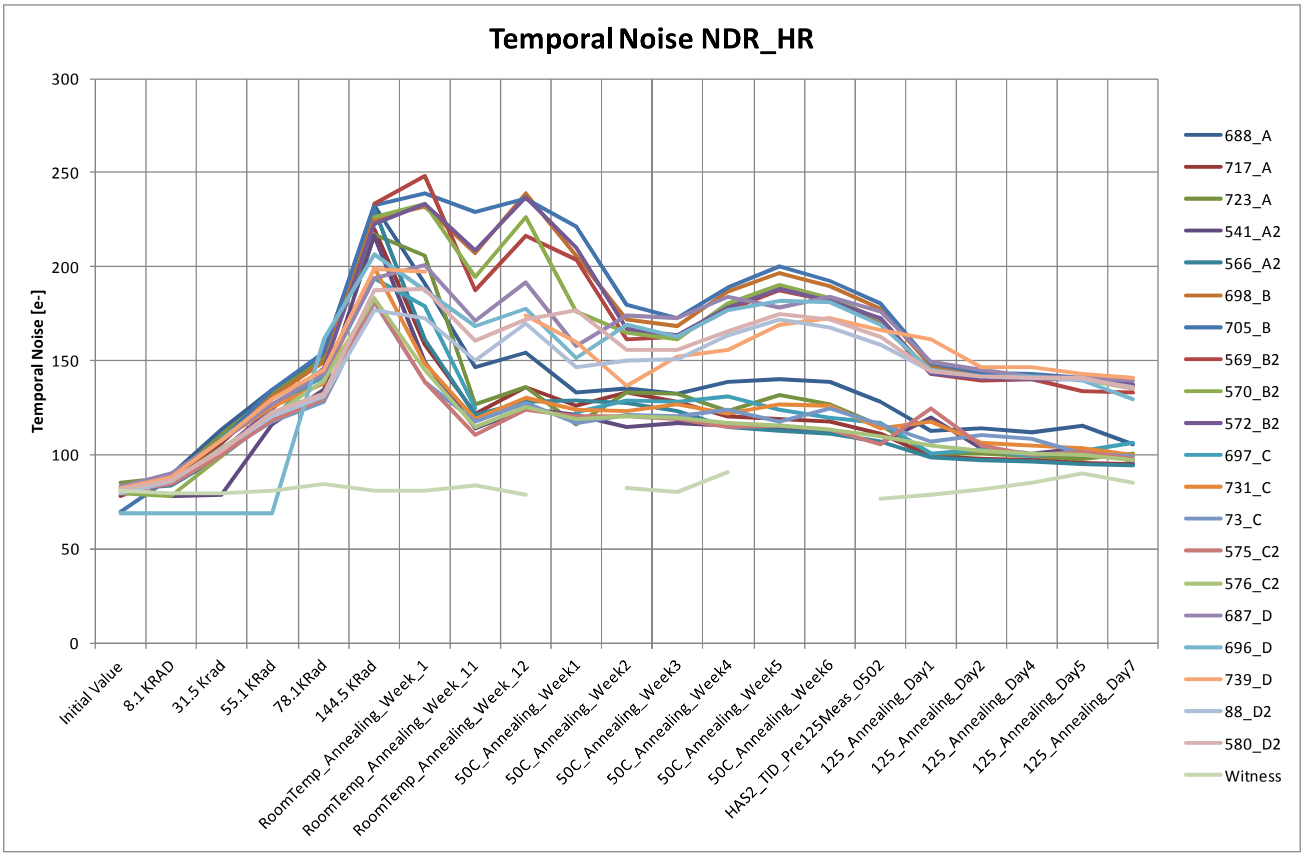


**Figure 8-8: Temporal Noise in NDR mode – hard reset vs radiation and annealing**

The following observations are made:

- Some test points are not reliable due to tester instability during the radiation test.
- Temporal noise is increasing with radiation. This is probably due to the 200ms minimal integration time on the tester. With increasing radiation a dark current component is added to the temporal noise. There is no difference in biasing scheme.
- Temporal noise is decreasing during room temperature annealing, though the parts which were in the ‘ON’ state are decreasing much faster and more homogenous than the ones which are annealed in the ‘OFF’ state. The same effect has been seen for the dark current.

### 8.2.5. Temporal Noise in NDR Mode – hard to soft reset

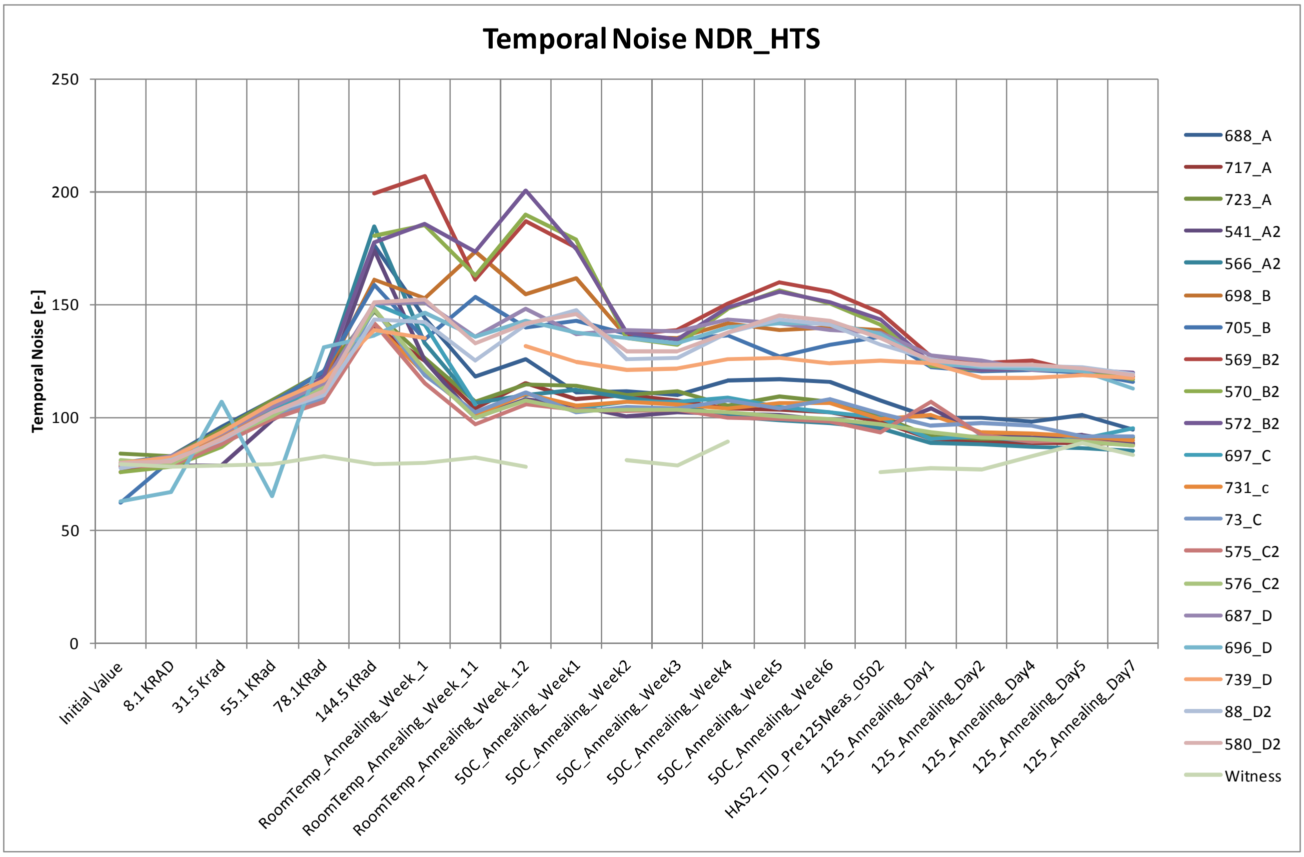


**Figure 8-9: Temporal Noise in NDR mode – hard to soft reset vs radiation and annealing**

The following observations are made:

- Some test points are not reliable due to tester instability during the radiation test.
- Temporal noise is increasing with radiation. This is probably due to the 200ms minimal integration time on the tester. With increasing radiation a dark current component is added to the temporal noise. There is no difference in biasing scheme.
- Temporal noise is decreasing during room temperature annealing, though the parts which were in the 'ON' state are decreasing much faster and more homogenous than the ones which are annealed in the 'OFF' state. The same effect has been seen for the dark current.

### 8.2.6. Global Fixed Pattern Noise – hard reset

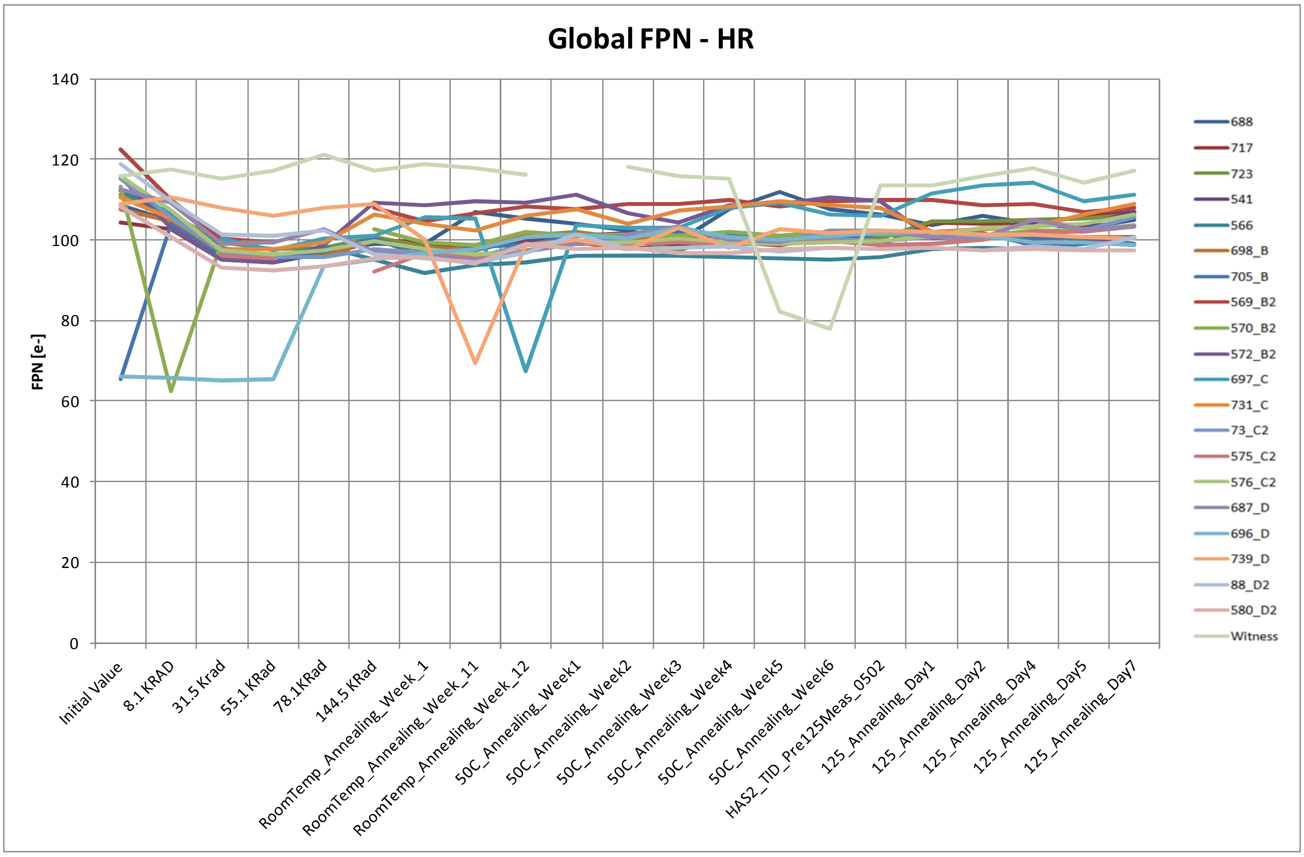


**Figure 8-10: Global FPN – hard reset vs radiation and annealing**

The following observations are made:

- Some test points are not reliable due to tester instability.
- Taking an average over the different samples, there's no difference visible between radiation, room temperature annealing and high temperature annealing.
- There is no clear difference between the different biasing schemes.

### 8.2.7. Global Fixed Pattern Noise – hard to soft reset

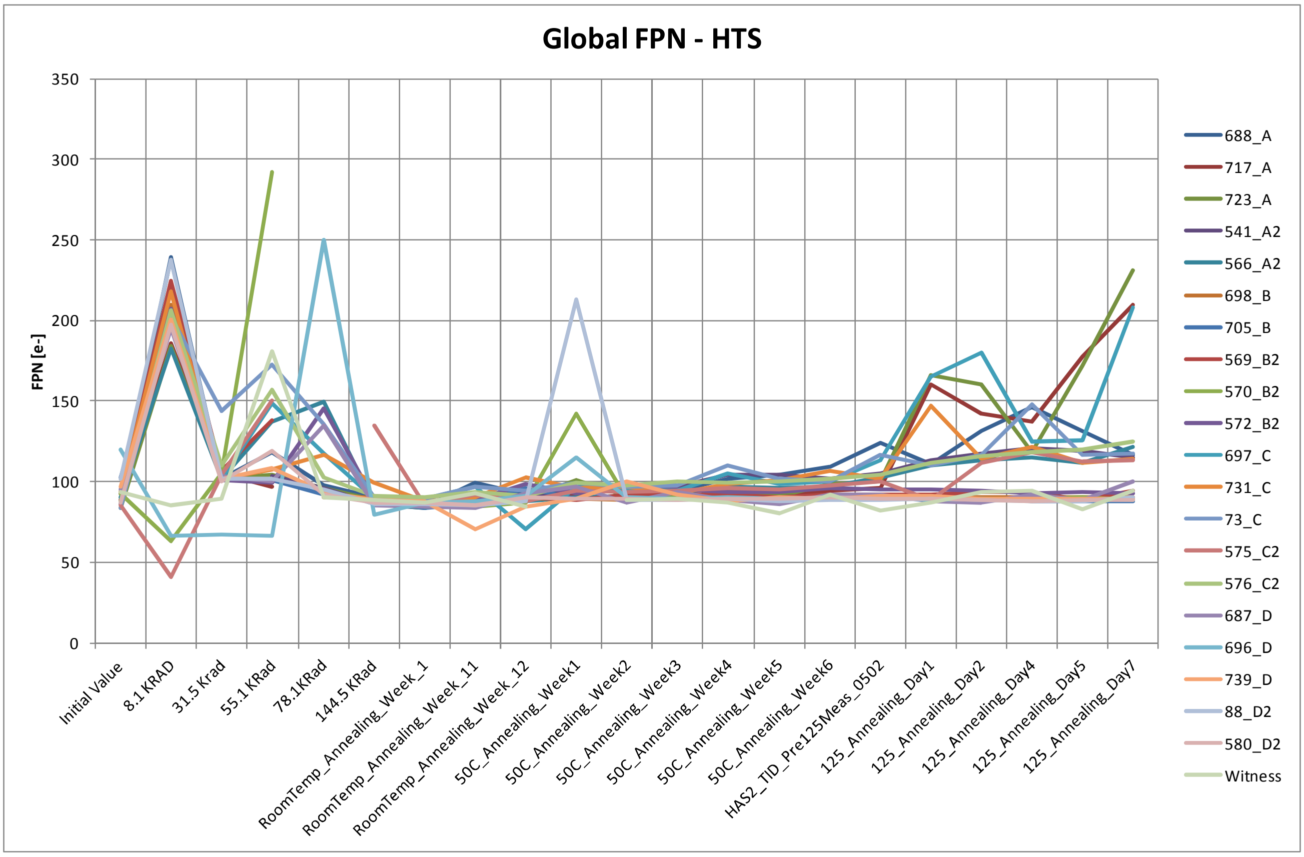


**Figure 8-11 Global FPN – hard to soft reset vs radiation and annealing**

The following observations are made:

- Some test points are not reliable due to tester instability, especially during radiation.
- The FPN, measured during high temperature annealing for the parts in the 'ON' condition, increases. This is the opposite effect of what has been observed with the dark current. Re-measurement of the parts 7 months later showed initial values again.

### 8.2.8. Local Fixed Pattern Noise – hard reset

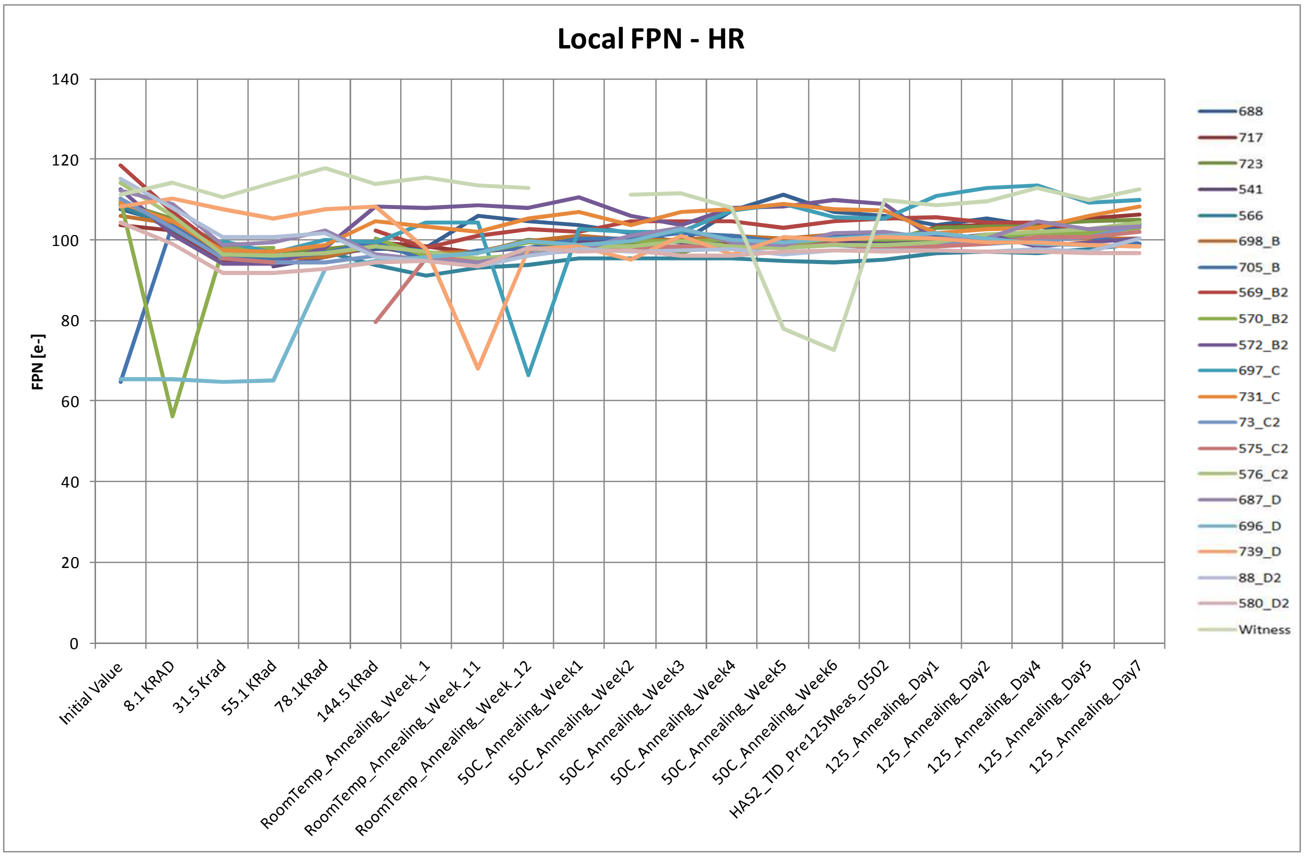


**Figure 8-12 Local FPN – hard reset vs radiation and annealing**

- Some test points are not reliable due to tester instability.
- Taking an average over the different samples, there's no difference visible between radiation, room temperature annealing and high temperature annealing.
- There is no clear difference between the different biasing schemes.
- FPN is decreasing with increasing radiation. The same observation was made during the evaluation campaign in 2007.

### 8.2.9. Local Fixed Pattern Noise – hard to soft reset

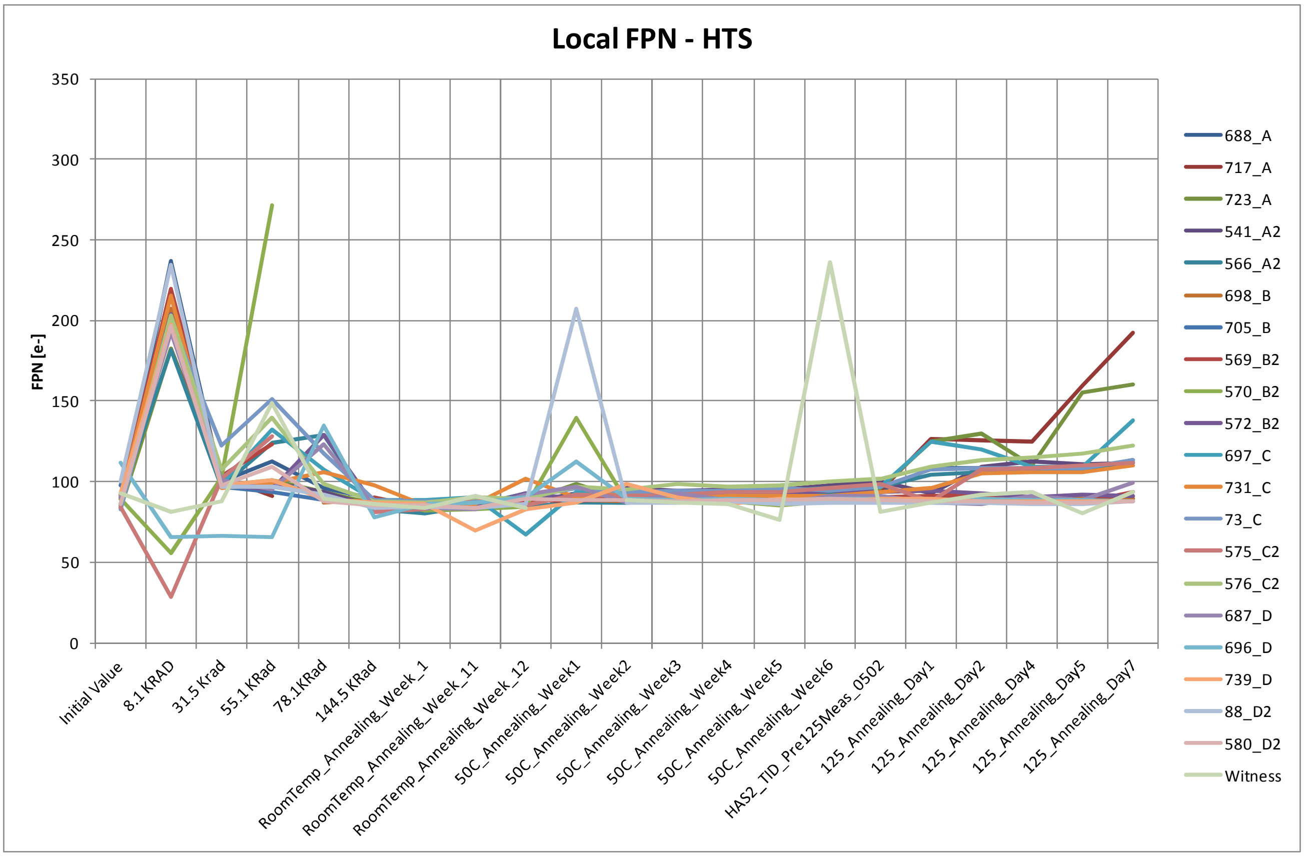


**Figure 8-13: Local FPN – hard to soft reset vs radiation and annealing**

- Some test points are not reliable due to tester instability, especially during radiation.
- The FPN, measured during high temperature annealing for the parts in the 'ON' condition, increases. This is the opposite effect of what has been observed with the dark current. Re-measurement of the parts 7 months later showed normal values again.

### 8.2.10. Global Photo Response Non Uniformity

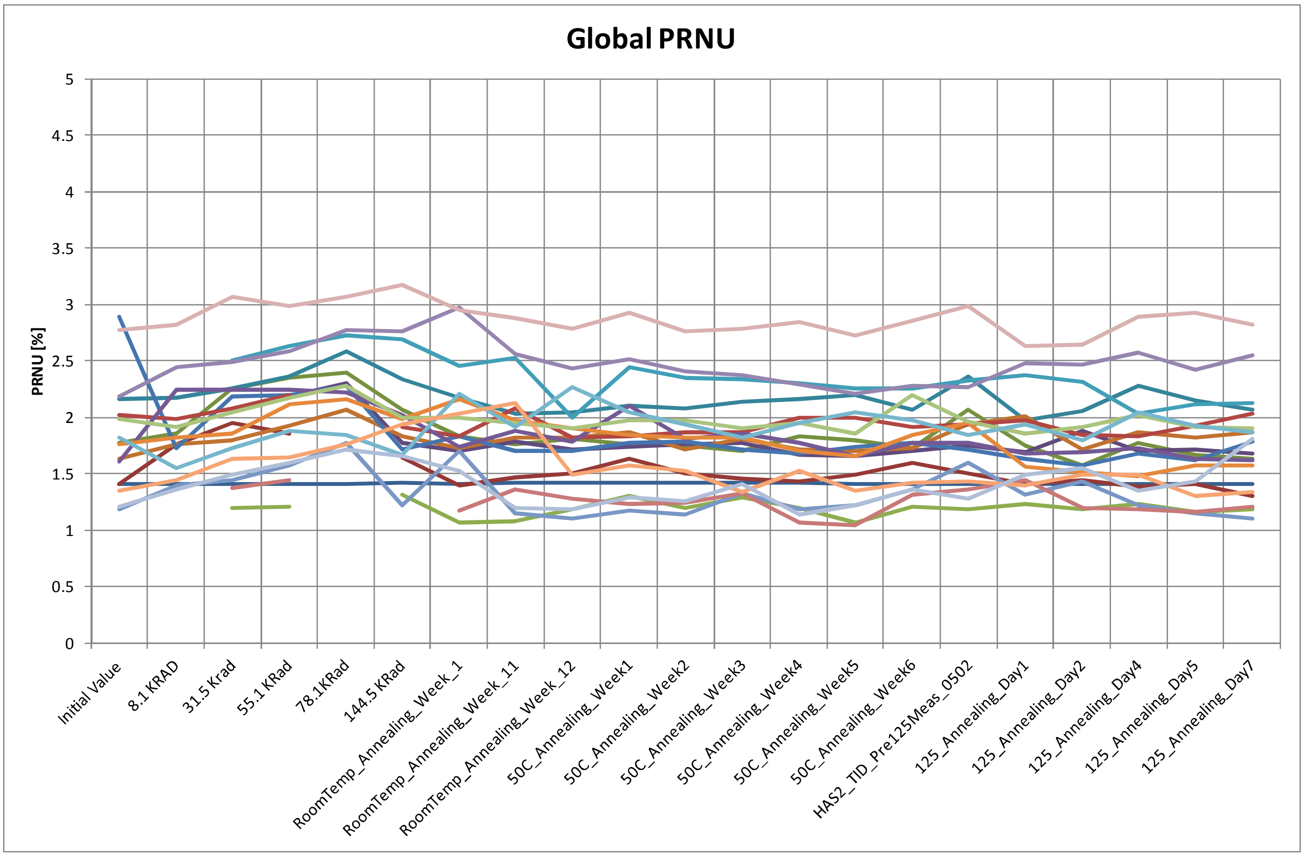


**Figure 8-14: Global PRNU vs radiation and annealing**

- There's no drift visible during radiation or during room temperature and high temperature annealing.
- The fluctuations visible are probably due to some influence of particle and handling contamination as the tests were performed in non clean room environment.

### 8.2.11. Local Photo Response Non Uniformity

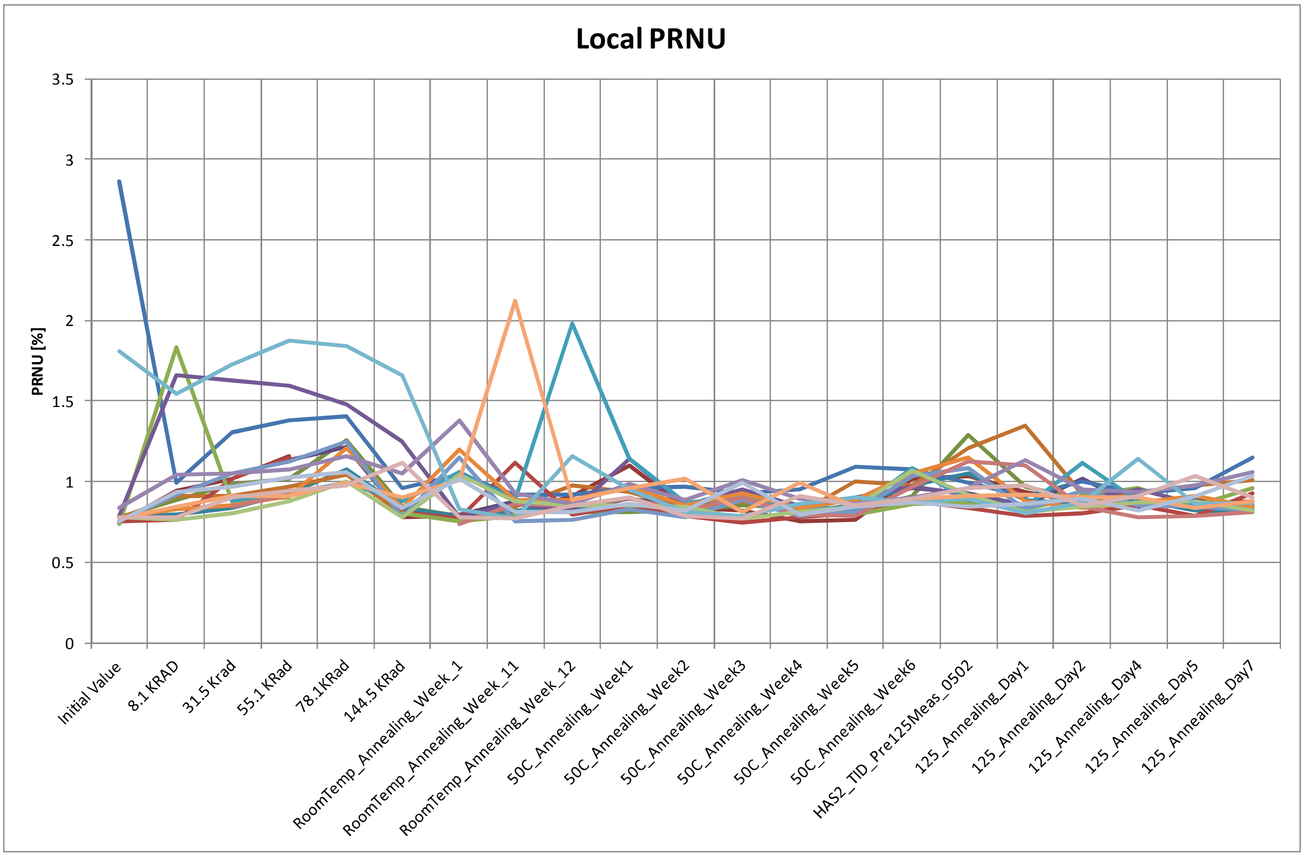


**Figure 8-15: Local PRNU vs radiation and annealing**

- There’s some fluctuation visible during radiation. This is probably due to the instability of the tester.
- There’s no drift visible during room temperature and high temperature annealing.

## 8.2.12. Operating Current

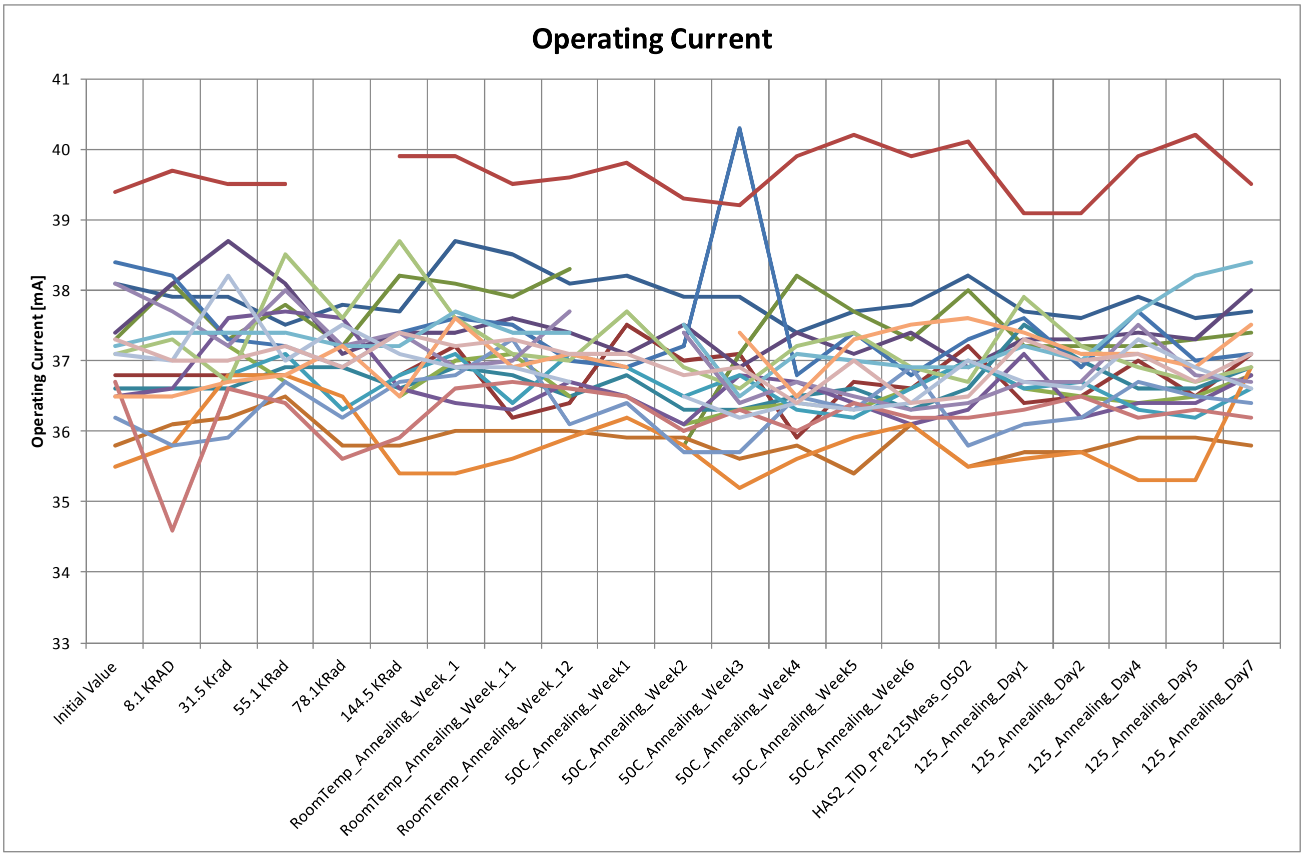


**Figure 8-16: Operating Current vs radiation and annealing**

- The operation current does not change over radiation, room temperature annealing and high temperature annealing. Also the different biasing schemes have no influence.

## 8.2.13. Standby Current

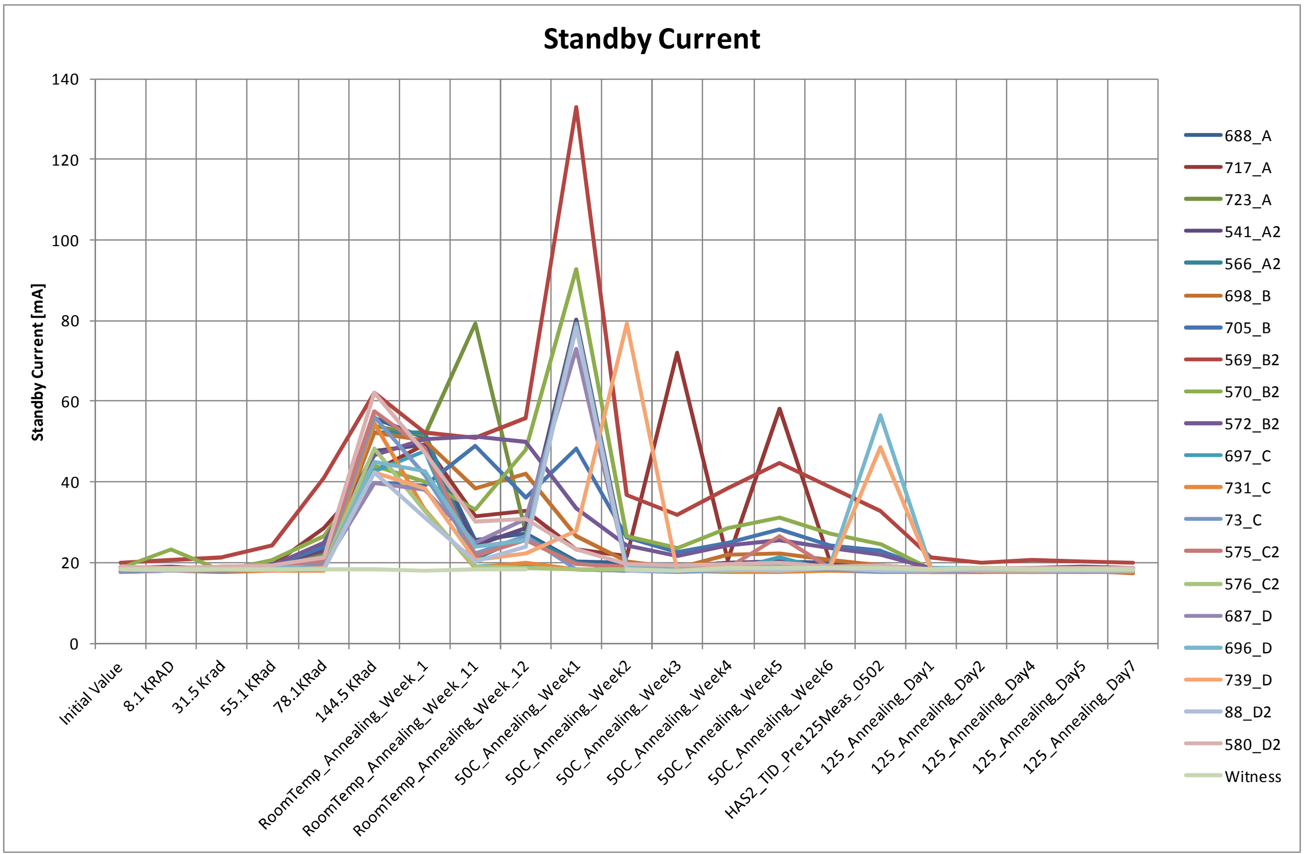


**Figure 8-17: Standby Current vs radiation and annealing**

- Standby current is getting unstable after the 78.1KRad measurement point. The same observation was made during the evaluation phase in 2007, though the effect was only seen at elevated temperature (85 degC).

- Standby current keeps unstable during room temperature annealing and 50 degrees annealing. The majority of the devices showing unstable behavior are annealed in the 'OFF' state.

- Standby current gets back to normal during high temperature annealing.

### 8.2.14.DSNU

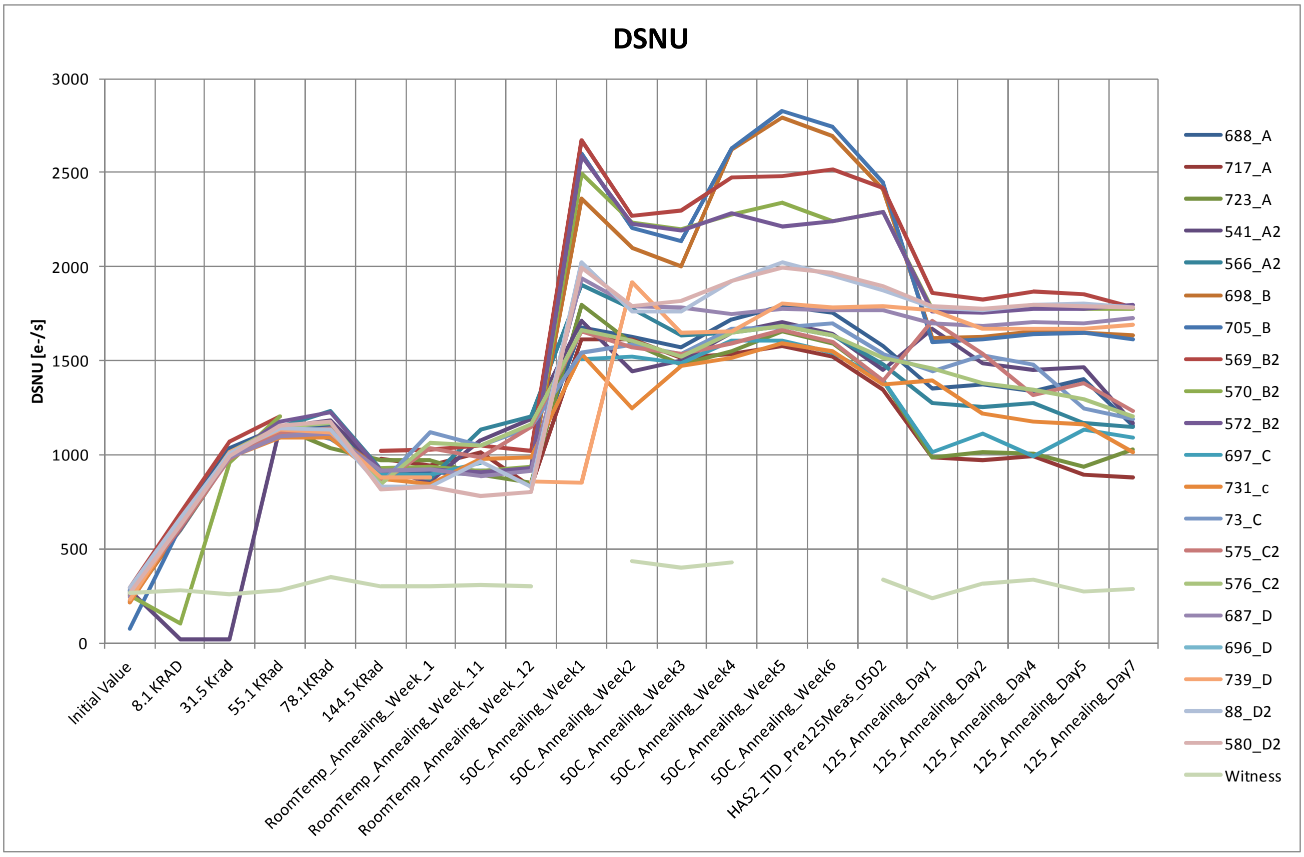


**Figure 8-18: DSNU vs radiation and annealing**

- DSNU increases the same for all the samples, independent from the wafer lot, independent from the biasing conditions
- DSNU does not change significantly during room temperature annealing. No influence from the bias condition.
- DSNU increases significantly after 1 day of 50 degrees C annealing for the OFF biasing condition (B, B2, D and D2).
- DSNU drops during 125degC annealing for both the biased and unbiased condition.
- Some measurement points are unreliable due to tester instability.

## 8.2.15.INL

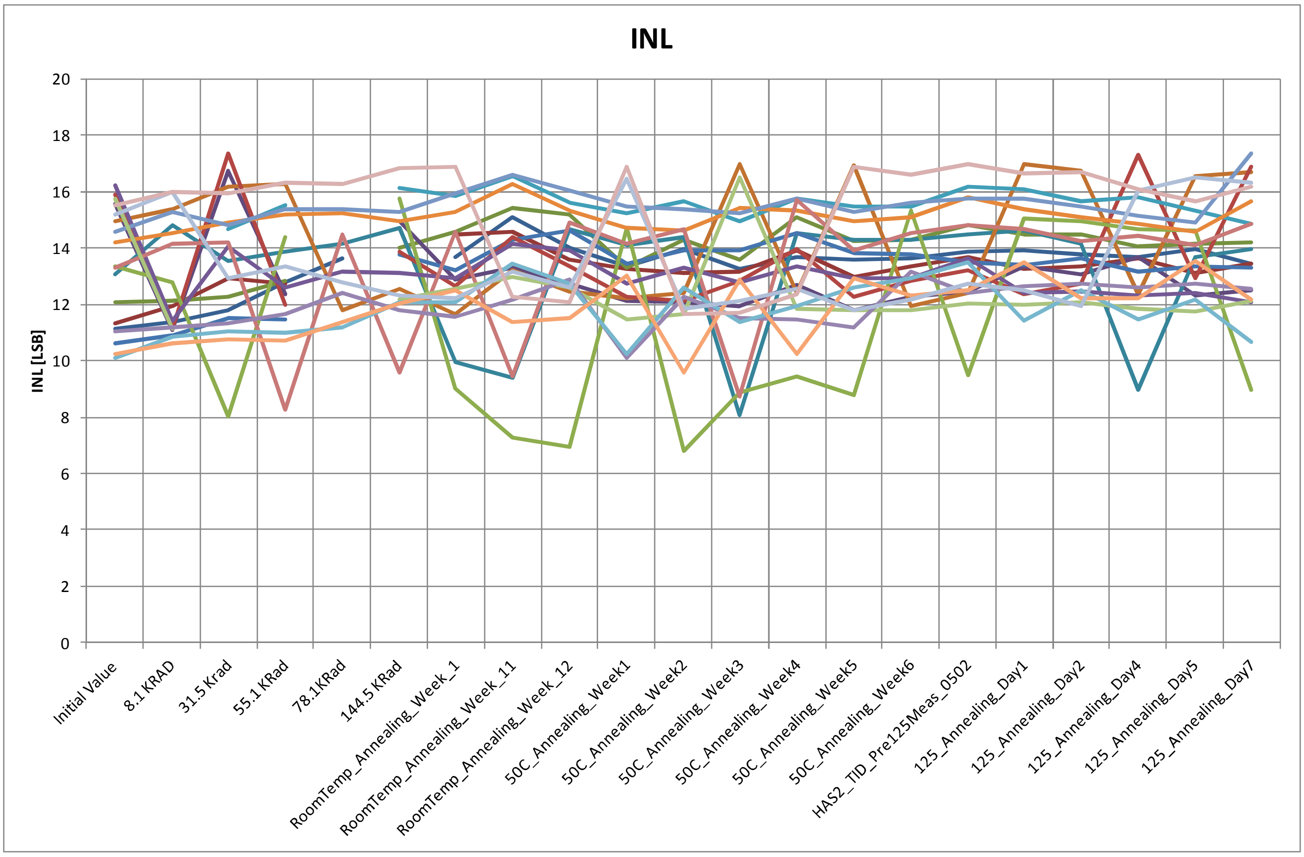


**Figure 8-19: INL vs radiation and annealing**

- INL is a very unstable measurement due to the behavior of the HAS2 ADC.
- There's no increase or decrease visible during radiation or annealing.

## 8.2.16.DNL

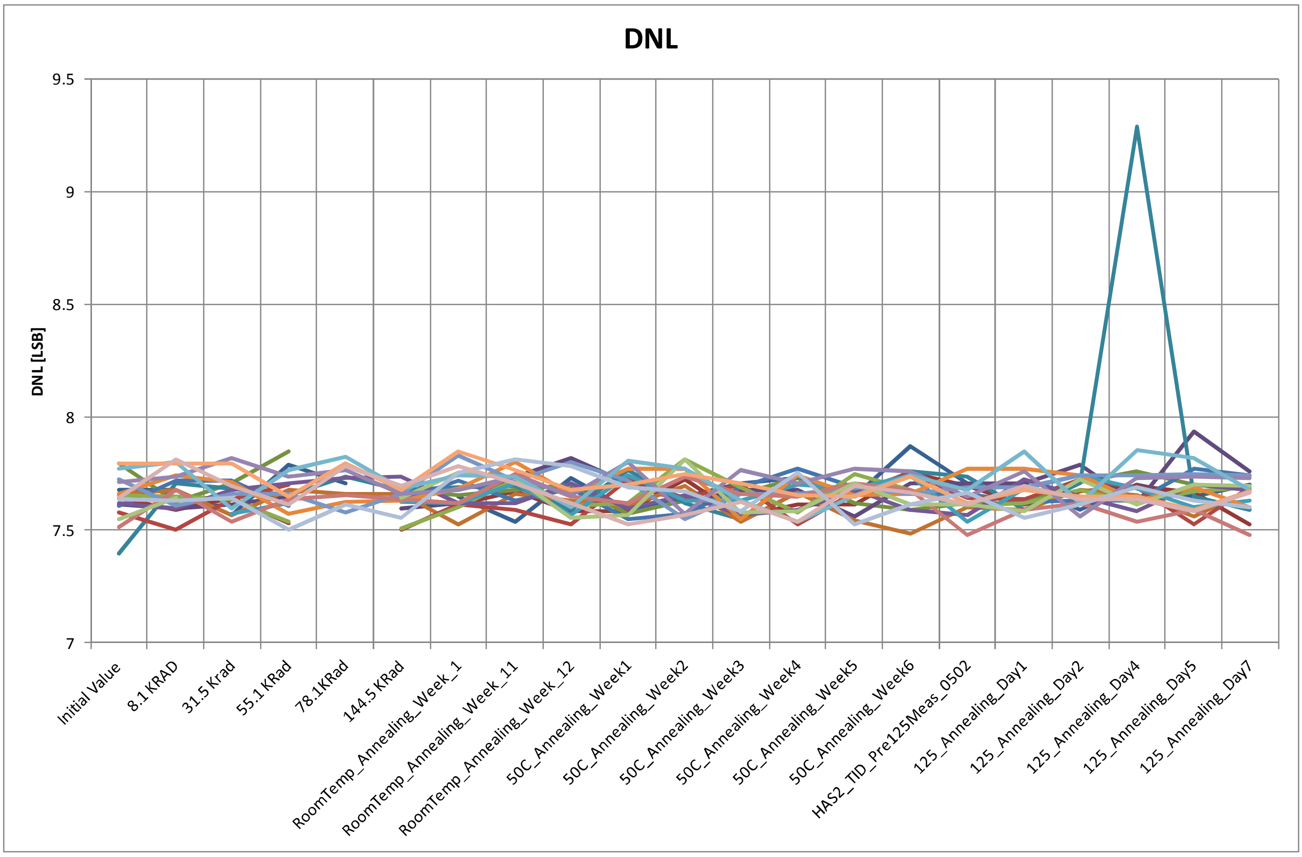


**Figure 8-20: DNL vs radiation and annealing**

- There's no increase or decrease visible during radiation or annealing.

### 8.2.17. Electro Optical Measurements

Electro optical measurements were performed on 5 devices. 2 Devices were selected from the new wafer lot; another 2 devices were selected from the same lot that was used for the evaluation campaign in 2007. Finally one device was used as a reference device.

| Device ID | Silicon Wafer Lot | Assembly Lot |
| --- | --- | --- |
| 689 | P29506.1 | 11-002 |
| 688 | P29506.1 | 11-002 |
| 073 | P20291.1 | ESA-QUAL-LOT |
| 088 | P20291.1 | ESA-QUAL-LOT |
| 164 | Reference Device | ESA-QUAL-LOT |

Observations:

- After radiation we were unable to retrieve data from device nr. 689. Also during the radiation campaign this device was not working properly. Analysis has shown that there was a broken lead on the device. This probably happened when inserting and taking out the device from its test socket.

- Device nr.88 was drawing a very high leakage current in the test pixel array and as such was not usable anymore for measuring spectral and optical response.

- Only device 688 and 73 could be measured after radiation.

8.2.17.1.Spectral Response

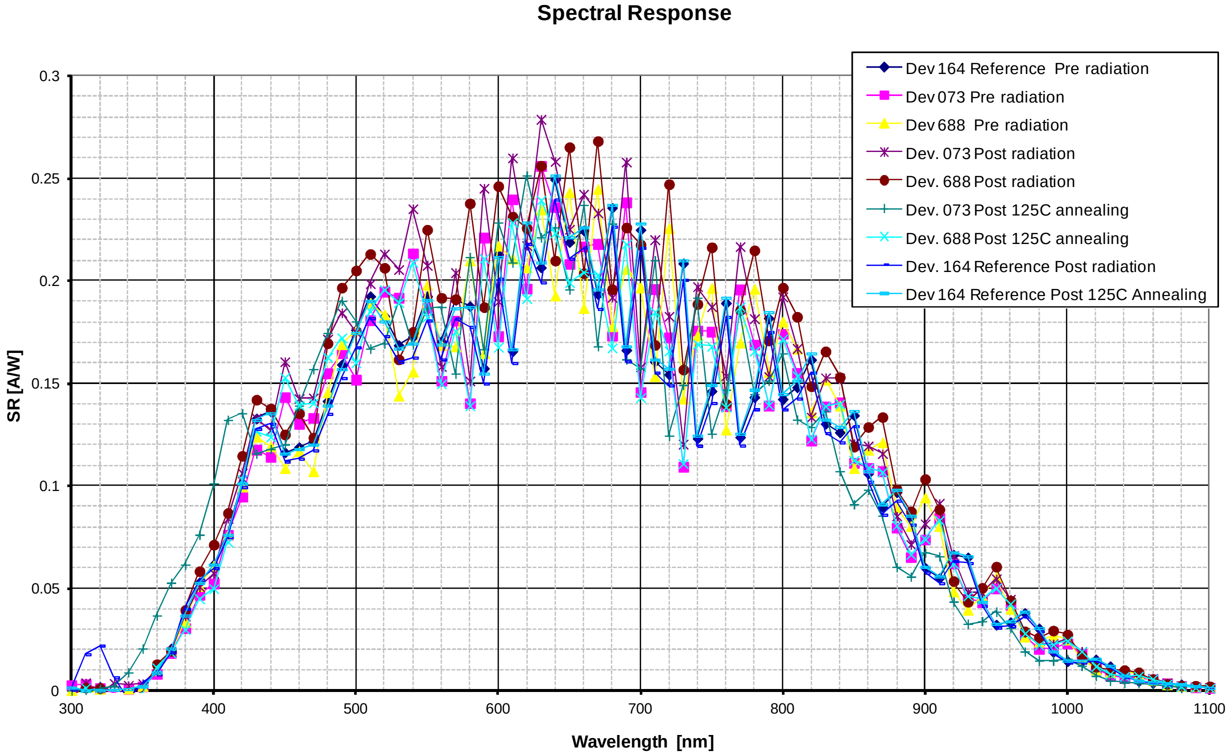


**Figure 8-21: Spectral Response before and after radiation and annealing**

No degradation is visible after 144KRad TID. The minor deviations that are visible are due to setup-to-setup variations.

| Response Data | | | |
|---|---|---|---|
| Device | Average Value 400-900 nm [A/W] Pre Radiation | Average Value 400-900 nm [A/W] Post Radiation | Average Value 400-900 nm [A/W] Post 125C Annealing |
| 073 | 0.158 | 0.173 | 0.155 |
| 688 | 0.159 | 0.177 | 0.162 |
| 164 | 0.157 | 0.150 | 0.157 |

### 8.2.17.2. Optical Response

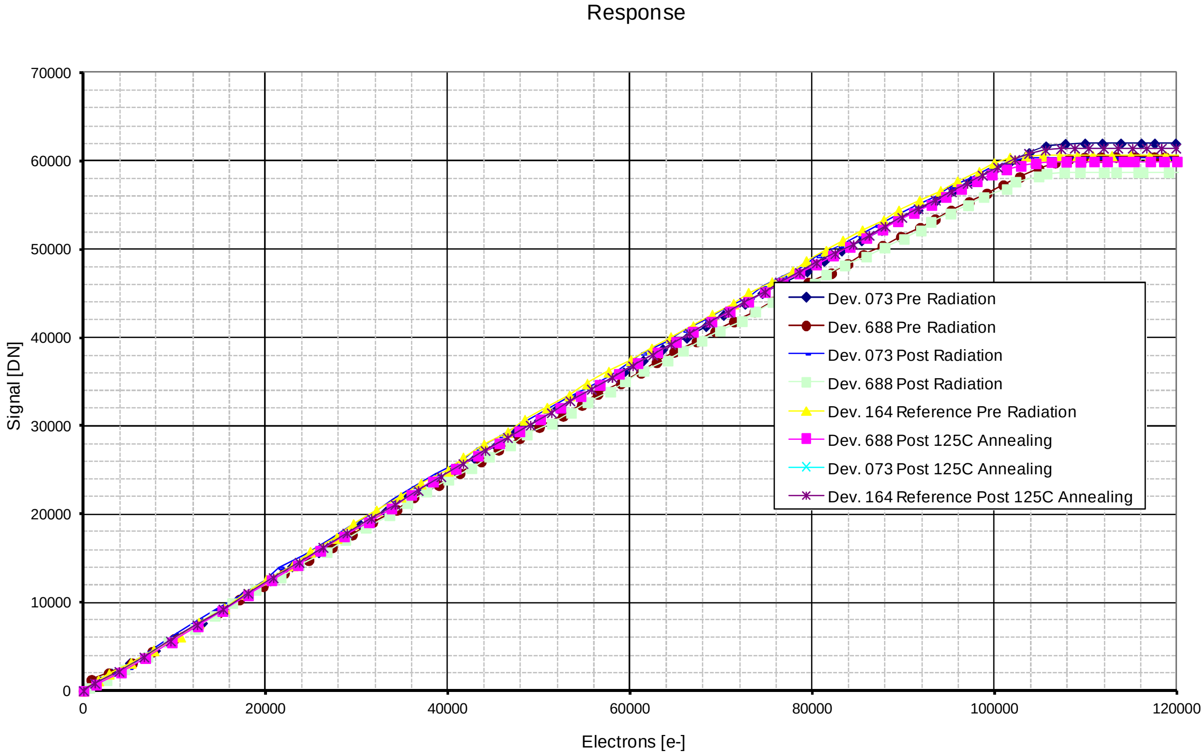


**Figure 8-22: Optical Response before and after radiation and annealing**

No degradation is visible after 144KRad TID. The minor deviations that are visible are due to setup-to-setup variations.

| Conversion Factor (CF) Data | | | |
| --- | --- | --- | --- |
| Device | CF [µV/e-] Pre Radiation | CF [µV/e-] Post Radiation | CF [µV/e-] Post 125C Annealing |
| 073 | 13.6 | 14.1 | 13.7 |
| 688 | 13.2 | 13.3 | 13.8 |
| 164 | 14.1 | 13.8 | 13.7 |

8.2.17.3.MTF

| MTF Data | | | |
|---|---|---|---|
| Device | MTF [%] Pre Radiation | MTF [%] Post Radiation | MTF [%] Post 125C Annealing |
| 073 | 43.9 | 39.3 | 39.8 |
| 088 | 37.7 | 40.7 | 38.2 |
| 688 | 41.7 | 37.9 | 36.8 |
| 164 | 42.9 | 40.24 | 42.8 |

The deviations are due to setup-to-setup variation.

8.2.17.4.Dark Signal Doubling Temperature

The dark signal doubling temperature was measured by placing the devices under a thermo stream. Temperatures used were 10ºC, 25ºC and 40ºC.

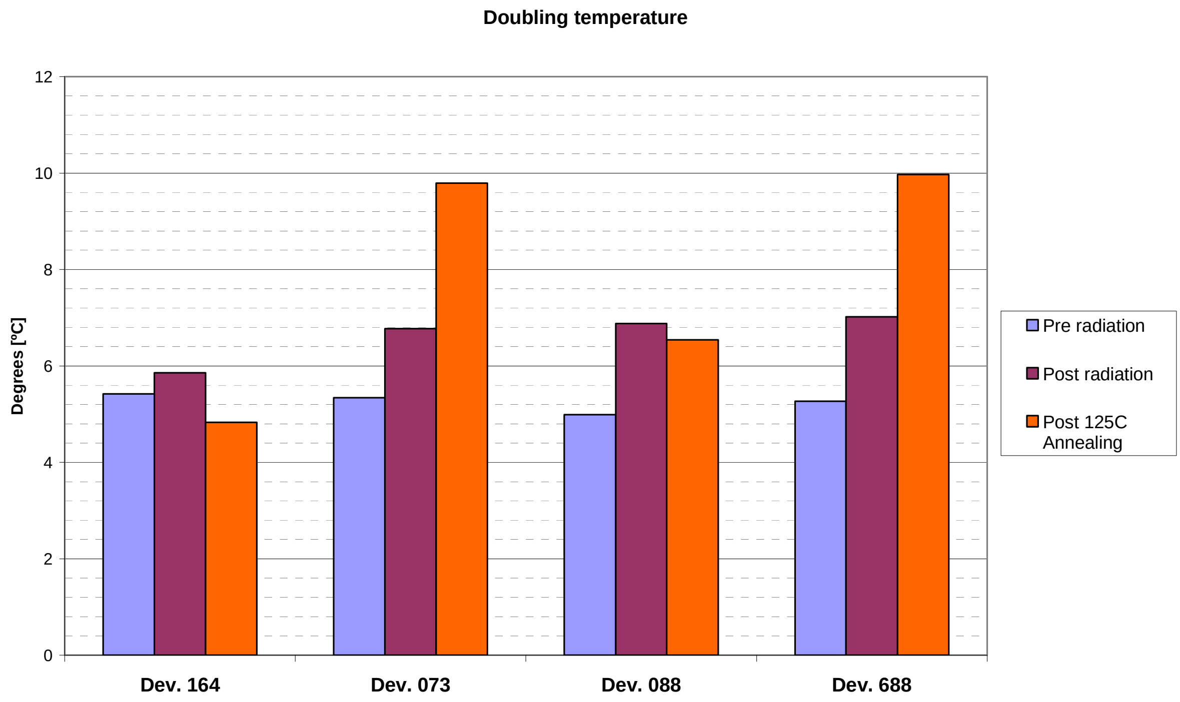


| Doubling Temperature | | | |
|---|---|---|---|
| Device | DT [ºC] Pre Radiation | DT [ºC] Post Radiation | DT [ºC] Post 125C Annealing |
| 073 | 5.34 | 6.78 | 9.79 |
| 088 | 4.99 | 6.88 | 6.54 |
| 688 | 5.27 | 6.88 | 9.97 |
| 164 | 5.42 | 5.86 | 4.93 |

Observations :

- Device. 088 behaves different compared to device 073 and 688. This might be related to the biasing state of the device during annealing. Device 088 is annealed in the ‘OFF’ state whereas device 73 and 688 are annealed in the ‘ON’ state.

- It is remarkable that the doubling temperature of device 688 and 073 is increasing even after high temperature annealing. At the moment of writing this test report no explanation can be given for this behavior.

8.2.17.5.Image Lag

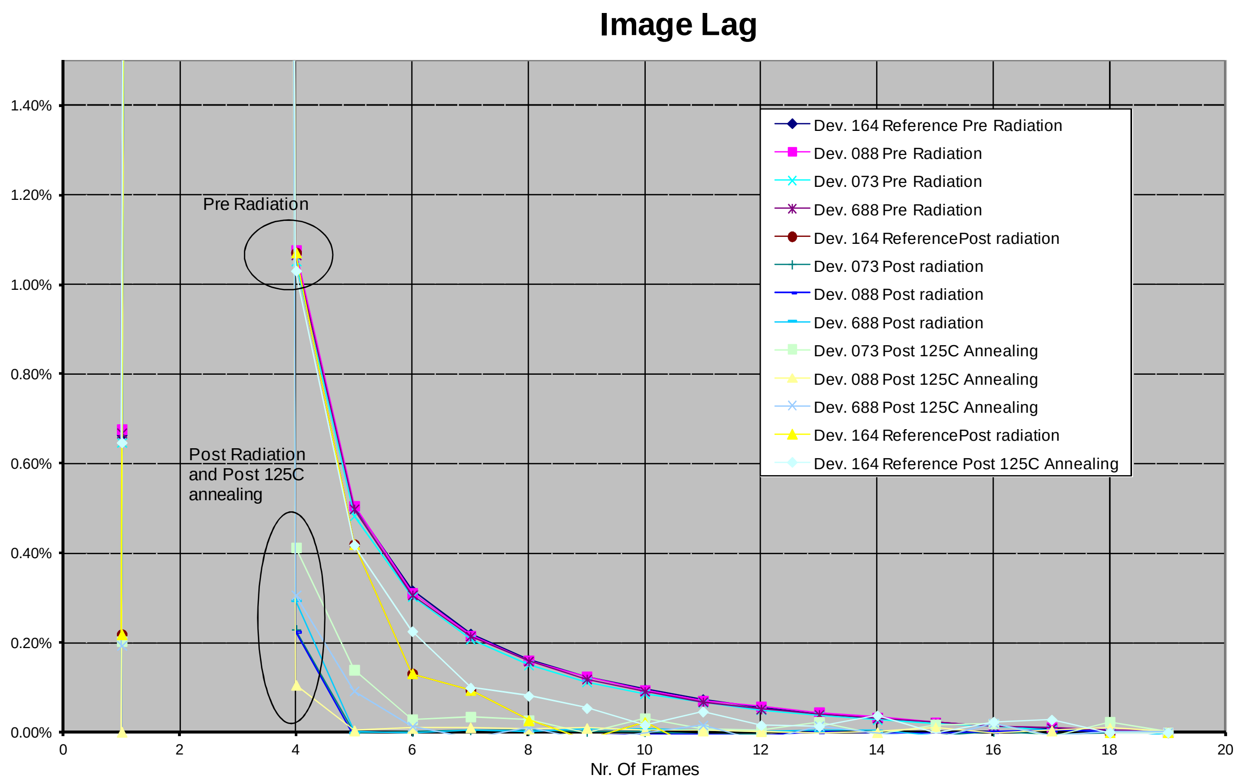


| Image Lag Data | | | |
|---|---|---|---|
| Device | Image Lag [%] Pre Radiation | Image Lag [%] Post Radiation | Image Lag [%] Post 125C Annealing |
| 073 | 1.05 | 0.23 | 0.41 |
| 088 | 1.08 | 0.22 | 0.11 |
| 688 | 1.07 | 0.30 | 0.31 |
| 164 | 1.07 | 1.07 | 1.03 |

The image lag for the reference device is stable for each measurement, confirming a proper setup. It is unknown why the image lag drops after radiation.

### 8.2.18.Calibration Parameters

Odd/even offset matching, NDR black level offset and temperature sensor curve calibration parameters were measured before and after radiation.

| Test | ID | Matchable | Value | | Black Offset/ Reg | Temp Calib | Voltage |
|---|---|---|---|---|---|---|---|
| PRE | 723 | 1 | 85 | 23.07 | 26 | 85 | 1.156 |
| | | | 84 | 11.51 | | -40 | 1.6844 |
| | | | 86 | 29.88 | | 25 | 1.4327 |
| POST | 723 | 1 | 89 | 4.51 | 24 | 85 | 1.1503 |
| | | | 88 | 11.85 | | -40 | 1.6931 |
| | | | 90 | 5.197 | | 25 | 1.4326 |
| PRE | 741 | Not Matchable | | | 29 | 85 | 1.1423 |
| | | | | | | -40 | 1.6637 |
| | | | | | | 25 | 1.4144 |
| POST | 741 | Not Matchable | | | 27 | 85 | 1.1538 |
| | | | | | | -40 | 1.6682 |
| | | | | | | 25 | 1.4186 |
| PRE | 713 | Not Matchable | | | 25 | 85 | 1.1101 |
| | | | | | | -40 | 1.6613 |
| | | | | | | 25 | 1.4007 |
| POST | 713 | Not Matchable | | | 23 | 85 | 1.1219 |
| | | | | | | -40 | 1.665 |
| | | | | | | 25 | 1.4055 |
| PRE | 717 | 1 | 85 | 11.14 | 28 | 85 | 1.1449 |
| | | | 84 | 18.38 | | -40 | 1.6744 |
| | | | 86 | 0.8134 | | 25 | 1.4225 |
| POST | 717 | 1 | 94 | 17.08 | 26 | 85 | 1.1108 |
| | | | 93 | 24.36 | | -40 | 1.6421 |
| | | | 95 | 9.302 | | 25 | 1.3815 |
| PRE | 705 | Not Matchable | | | 26 | 85 | 1.1327 |
| | | | | | | -40 | 1.6703 |
| | | | | | | 25 | 1.4155 |
| POST | 705 | Not Matchable | | | 24 | 85 | 1.1195 |
| | | | | | | -40 | 1.7078 |
| | | | | | | 25 | 1.4357 |
| PRE | 679 | 1 | 54 | 11.35 | 26 | 85 | 1.1331 |
| | | | 53 | 17.28 | | -40 | 1.6726 |
| | | | 55 | 2.815 | | 25 | 1.4158 |
| POST | 679 | 1 | 58 | 13.77 | 24 | 85 | 1.1377 |
| | | | 57 | 24.03 | | -40 | 1.6751 |
| | | | 59 | 8.682 | | 25 | 1.4174 |
| PRE | 698 | 1 | 49 | 1.434 | 29 | 85 | 1.1626 |
| | | | 48 | 8.9 | | -40 | 1.6849 |
| | | | 50 | 8.575 | | 25 | 1.4335 |
| POST | 698 | 1 | 39 | 4.927 | 27 | 85 | 1.1388 |
| | | | 38 | 4.396 | | -40 | 1.6856 |
| | | | 40 | 13.21 | | 25 | 1.3664 |

| Test | ID | Matchable | Value | | Black Offset/ Reg | Temp Calib | Voltage |
|---|---|---|---|---|---|---|---|
| PRE | 697 | 1 | 88 | 18.86 | 34 | 85 | 1.1315 |
| | | | 87 | 28.15 | | -40 | 1.6645 |
| | | | 89 | 9.744 | | 25 | 1.4107 |
| POST | 697 | 1 | 93 | 6.417 | 31 | 85 | 1.1305 |
| | | | 92 | 15.77 | | -40 | 1.6642 |
| | | | 94 | 0.9434 | | 25 | 1.4126 |
| PRE | 731 | 1 | 102 | 11.08 | 29 | 85 | 1.1315 |
| | | | 101 | 19.15 | | -40 | 1.6673 |
| | | | 103 | 0.1161 | | 25 | 1.4111 |
| POST | 731 | 1 | 114 | 3.779 | 26 | 85 | 1.1138 |
| | | | 113 | 7.943 | | -40 | 1.6227 |
| | | | 115 | 8.253 | | 25 | 1.3674 |
| PRE | 739 | Not Matchable | | | 33 | 85 | 1.1272 |
| | | | | | | -40 | 1.6566 |
| | | | | | | 25 | 1.4047 |
| POST | 739 | Not Matchable | | | 29 | 85 | 1.0927 |
| | | | | | | -40 | 1.6444 |
| | | | | | | 25 | 1.3961 |
| PRE | 687 | Not Matchable | | | 33 | 85 | 1.1181 |
| | | | | | | -40 | 1.6605 |
| | | | | | | 25 | 1.4031 |
| POST | 687 | Not Matchable | | | 30 | 85 | 1.1107 |
| | | | | | | -40 | 1.6437 |
| | | | | | | 25 | 1.3844 |
| PRE | 696 | 1 | 203 | 0.07455 | 35 | 85 | 1.1369 |
| | | | 202 | 10.04 | | -40 | 1.6693 |
| | | | 204 | 6.391 | | 25 | 1.4164 |
| POST | 696 | 1 | 227 | 7.355 | 33 | 85 | 1.1122 |
| | | | 226 | 0.1672 | | -40 | 1.6526 |
| | | | 228 | 16.89 | | 25 | 1.3959 |
| PRE | 689 | Not Matchable | | | 28 | 85 | 1.1435 |
| | | | | | | -40 | 1.6678 |
| | | | | | | 25 | 1.4345 |
| POST | 689 | Not Matchable | | | 26 | 85 | 1.1674 |
| | | | | | | -40 | 1.682 |
| | | | | | | 25 | 1.4358 |
| PRE | 688 | Not Matchable | | | 35 | 85 | 1.1324 |
| | | | | | | -40 | 1.6605 |
| | | | | | | 25 | 1.4097 |
| POST | 688 | Not Matchable | | | 30 | 85 | 1.1429 |
| | | | | | | -40 | 1.6639 |
| | | | | | | 25 | 1.4129 |
| PRE | 541 | 1 | 26 | 2.807 | 47 | 85 | 1.1544 |
| | | | 25 | 11.15 | | -40 | 1.667 |
| | | | 27 | 5.185 | | 25 | 1.4138 |
| POST | 541 | 1 | 40 | 15.83 | 44 | 85 | 1.1262 |
| | | | 39 | 5.005 | | -40 | 1.6532 |

| Test | ID | Matchable | Value | | Black Offset/ Reg | Temp Calib | Voltage |
|---|---|---|---|---|---|---|---|
| | | | 41 | 24.45 | | 25 | 1.4031 |
| | | | 208 | 4.874 | | 85 | 1.1565 |
| | | | 207 | 0.3598 | | -40 | 1.6575 |
| PRE | 566 | 1 | 209 | 10.29 | 41 | 25 | 1.4019 |
| | | | 189 | 22 | | 85 | 1.1134 |
| | | | 188 | 31.2 | | -40 | 1.6466 |
| POST | 566 | 1 | 190 | 17.02 | 38 | 25 | 1.3853 |
| | | | 108 | 15.63 | | 85 | 1.1549 |
| | | | 107 | 4.461 | | -40 | 1.6512 |
| PRE | 569 | 1 | 109 | 23.8 | 48 | 25 | 1.4061 |
| | | | 89 | 5.104 | | 85 | 1.1208 |
| | | | 88 | 13 | | -40 | 1.6451 |
| POST | 569 | 1 | 90 | 0.5822 | 46 | 25 | 1.4022 |
| | | | 67 | 46.58 | | 85 | 1.1555 |
| | | | 66 | 36.25 | | -40 | 1.6639 |
| PRE | 570 | 1 | 68 | 54.74 | 38 | 25 | 1.4142 |
| | | | 56 | 18.55 | | 85 | 1.1259 |
| | | | 55 | 29.92 | | -40 | 1.6711 |
| POST | 570 | 1 | 57 | 9.716 | 36 | 25 | 1.4188 |
| | | | 162 | 15.72 | | 85 | 1.1614 |
| | | | 161 | 20.59 | | -40 | 1.6785 |
| PRE | 572 | 1 | 163 | 7.177 | 43 | 25 | 1.4298 |
| | | | 160 | 63.16 | | 85 | 1.1138 |
| | | | 159 | 72.19 | | -40 | 1.6421 |
| POST | 572 | 1 | 161 | 53.41 | 41 | 25 | 1.4012 |
| | | | 64 | 16.95 | | 85 | 1.1556 |
| | | | 63 | 25.67 | | -40 | 1.6598 |
| PRE | 576 | 1 | 65 | 6.791 | 44 | 25 | 1.4079 |
| | | | 45 | 42.53 | | 85 | 1.1125 |
| | | | 44 | 51.26 | | -40 | 1.66 |
| POST | 576 | 1 | 46 | 33.25 | 42 | 25 | 1.4012 |
| | | | 23 | 0.697 | | 85 | 1.1552 |
| | | | 22 | 8.515 | | -40 | 1.6714 |
| PRE | 580 | 1 | 24 | 7.288 | 41 | 25 | 1.4218 |
| | | | 19 | 2.93 | | 85 | 1.1021 |
| | | | 18 | 10.23 | | -40 | 1.6417 |
| POST | 580 | 1 | 20 | 6.576 | 38 | 25 | 1.3957 |
| | | | 118 | 0.6458 | | 85 | 1.1163 |
| | | | 117 | 9.812 | | -40 | 1.653 |
| PRE | 73 | 1 | 119 | 10.52 | 48 | 25 | 1.3965 |
| | | | 118 | 0.6458 | | 85 | 1.1163 |
| | | | 117 | 9.812 | | -40 | 1.653 |
| POST | 73 | 1 | 119 | 10.52 | 48 | 25 | 1.3965 |
| | | Not Matchable | | | | 85 | 1.1256 |
| | | | | | | -40 | 1.6565 |
| PRE | 88 | | | | 48 | 25 | 1.4035 |
| POST | 88 | Not Matchable | | | 46 | 85 | 1.1178 |

| Test | ID | Matchable | Value | Black Offset/ Reg | Temp Calib | Voltage |
|---|---|---|---|---|---|---|
| | | | | | -40 | 1.6211 |
| | | | | | 25 | 1.3829 |

Observations:

- There is a difference in register setting for the odd/even column matching in DR mode before and after radiation. The same observation was already made during the evaluation campaign in 2007. (ref. HAS Low Dose Rate radiation Test Report ESA/ESTEC/TEC-ECC/09.07/LS). The same variations were measured after annealing.

- There is a small difference noticeable for the NDR black offset parameter. As this test is done manually the small difference is probably due to test-to-test variation.

- The on-chip temperature diode is unaffected after radiation.

## 9.CONCLUSIONS

The HAS2 image sensor has been irradiated till 144 KRad using different biasing schemes. After radiation the devices were annealed for 3 months at room temperature, 1 month at 50 degC and 1 week at 125 degC. Annealing was also done using different biasing schemes.

From the observations the main conclusions are:

- There is no difference observed in dark current increase between sensors that are being biased (operational) and sensors that are in the off state (all pins grounded).

- During 50degC annealing, dark current is increasing on those sensors which are in the off state.

- During 125degC annealing, dark current is decreasing on all the parts.

- The dark current doubling temperature is increasing on those parts which are annealed in the ON state. The ones annealed in the off state do not show an increase.

- There is no difference between devices from different diffusion lots.